Available online at www.CivileJournal.org

Civil Engineering Journal

(E-ISSN: 2476-3055; ISSN: 2676-6957)

Vol. 11, No. 01, January, 2025

Shape Functions Development for Beam-Column Element with Semi-Rigid Connections in Second-Order Steel Frame Analysis

Quoc Anh Vu [1], Bao Trung Le Dung [1], Hai Quang Nguyen [2*]

[1] Faculty of Civil Engineering, Hanoi Architectural University, Ha Noi, Viet Nam.

[2] Faculty of Mechanical-Automotive and Civil Engineering, Electric Power University, Ha Noi, Viet Nam.

Received 03 October 2024; Revised 15 December 2024; Accepted 23 December 2024; Published 01 January 2025

Abstract

The objective of this paper is to provide a novel method for developing the shape functions of a beam-column element with semi-rigid connection ends, thereby establishing a static analysis method for semi-rigid steel frames. This method takes into account the influence of the P-Delta effect, according to the finite element method based on displacement (FEM). The shape function is established directly from a third-order Hermitian displacement function polynomial combined with the bending element deflection differential equation. The linear elastic stiffness matrix, the geometric stiffness matrix of a semi-rigid connection beam-column, and the equilibrium equation of the element in a local coordinate system are simultaneously obtained by applying Castigliano's theorem (Part 1) for elastic deformation potential energy expression. The computational program was developed using Matlab software, and the calculation results are verified against published research results, showing that the derived shape functions and the steel frame analysis method are reliable and trustworthy. In addition, this article also derives stiffness matrices and an equivalent nodal load vector for specific cases where the semi-rigid connection is fully rigid (FR) or a pin connection. The derived shape functions are polynomial expressions with coefficients that are simply calculated from the connection stiffness and the geometric and material characteristics of the element, making them highly convenient to use.

Keywords: Steel Frames; Beam-Column Element; Semi-Rigid Connection; Shape Functions; Second-Order Static Analysis.

1. Introduction

Steel frames are one of the main types of load-bearing structures, and they are often used in high-rise construction projects. Due to the characteristics of manufacturing and erecting steel frames using the assembly method, beam joints, column joints, column bases joints, and especially beam-column joints are often semi-rigid connections. Studies on the analysis of semi-rigid steel frames, including those by Stelmack (1982) [1], Chen & Lui (1987) [2], Anh (2003) [3], Quang (2012) [4], and Chan & Chui (2000) [5], have shown that semi-rigid connections play an important role in the behavior of frame structures. To obtain analysis results closer to the actual behavior of the frame structure and ensure an economy design, it is recommended in most cases to use a frame model with semi-rigid connections. In addition, steel frames often consist of slender components. Under applied loads, steel frames often experience lateral displacements and horizontal movement. At the same time, components sag, causing a significant impact on the performance of the frame. The effects due to such changes in geometry and loading are called P-Delta effects or second-order effects. Analysis that includes the P-Delta effect is also called second-order analysis. When the steel frames have semi-rigid connections, the P-Delta effect also changes the stiffness in the connections, leading to changes in the stiffness

* Corresponding author: quangnh@epu.edu.vn

http://dx.doi.org/10.28991/CEJ-2025-011-01-021

of the elements and the overall stiffness of the frame, thereby continuing to change the displacement and internal force of the frame. In fact, design standards such as AISC-LRFD (2000) [6] or Eurocode 3 (2005) [7] have provided formulas for determining the strength and stiffness of semi-rigid connections and regulations on calculating steel frames with semi-rigid connections as well as instructions on calculating steel frames considering the influence of P-Delta geometric nonlinearity. The existing literature shows that there are essentially seven methods to establish key quantities—such as the linear elastic stiffness matrix, geometric stiffness matrix, and equivalent nodal load vector—necessary for second-order analysis of semi-rigid steel frames. These methods can be summarized as follows:

***First method*:** Based on the "conjugate beam method", this approach deduces the relationship between force and displacement at the ends of the semi-rigid beam element, thereby building an elastic stiffness matrix for the semi-rigid beam-column element. This elastic stiffness matrix is presented as the elastic stiffness matrix of a beam-column element with both FR ends, multiplied by a correction matrix whose elements are functions of two parameters called the fixity factor. A notable contribution to this method was made by Monforton (1962) [8]. Due to the complexity of the expression, this method has not yet established the geometric stiffness matrix for the semi-rigid beam-column element. Consequently, some authors have combined it with the geometric stiffness matrix of the beam-column element with both FR ends for second-order analysis. Researchers such as Dhillon & Abdel-Majid (1990) [9], Xu & Grierson (1993) [10], and Xu (2001) [11] have utilized this approach.

***Second method*:** This method considers the rotating spring as a separate element and assembles it into the FR ends beam element to form a hybrid element, that is, the semi-rigid beam element. The main concept of this method is that the "internal moment" (on the spring side connected to the beam) and the "external moment" (on the spring side connected to the column) for each spring are balanced; and it is necessary to shorten the "free internal displacements" corresponding to the "internal moments" of the relationship between the moment, stiffness, and rotation angle of the hybrid element. The stiffness of the hybrid element is obtained by directly adding the stiffness of the corresponding connections to the bending stiffness in the elastic stiffness matrix of the double-end FR beam element. Lui & Chen (1985) [12] presented this method early on, and it is widely used in first-order analysis. Xu (1992) [13] assembled a rotating spring element into a FR double-end beam-column element to establish the stiffness matrix of the semi-rigid beam-column element, which includes a linear elastic stiffness matrix and a geometric stiffness matrix, which is used in second-order analysis. Researchers such as Chan & Chui (2000) [5], Chen (2000) [14], and Xu (2001) [11] have employed this method.

***Third method*:** This approach adjusts the rotation angle of the beam ends in the slope-deflection expression of the FR double-ended beam-column element, without relative horizontal displacement between the ends, to consider the presence of a semi-rigid connection and relative horizontal displacement between the ends. According to Bažant & Cedolin (2010) [15], the slope-deflection expression represents the moment-rotation angle relationship (when there is no relative horizontal displacement between the ends) at the two ends of the beam-column element, with parameters defined as stability functions located in a square matrix of size 2´2, as introduced by James (1935), in work related to the moment distribution method. Chen & Lui (1987) [2] divided frame elements into two types: semi-rigid beam-column elements and double-end FR column elements. The stiffness matrix of the semi-rigid beam-column element, whose coefficients are stability functions, is established considering the effects of both the semi-rigid connection and relative horizontal displacement between ends. When the effect of longitudinal force in this matrix is ignored, the stiffness matrix of the semi-rigid beam element is obtained. The stiffness matrix of the column element with two FR ends, whose coefficients are stability stiffness functions, is established to consider only the relative horizontal displacement of the ends without considering the influence of semi-rigid connections. The stability stiffness functions are complicated when they must be divided into two forms: the trigonometric functions for compressive axial force and the hyperbolic functions for tensile axial force. When the axial force is small (close to zero), the stability stiffness functions may become numerically unstable. The general method to handle transcendental functions in such cases is to expand them in series form, retaining the first two or three terms to return to the polynomial functions. This method was established by Chen & Lui (1987) [2], and it has been published in many documents. It is widely used in design guidelines according to American standards and cited by many authors in their research. These researchers include Dhillon & O'Malley III (1999) [16], Kim & Choi (2001) [17], and Nguyen & Kim (2014) [18].

***Fourth method*:** Similarly to Chen & Lui (1987) [2], but Quang (2012) [4] adjusted the rotation angle at beam ends in the formula to represent the horizontal displacement function according to third-order Hermitian shape functions and the nodal displacement vector of the beam element with both FR ends. This approach directly establishes the linear elastic stiffness matrix, mass matrix, and equivalent nodal load vector of the semi-rigid beam-column element for elastic-plastic analysis of semi-rigid steel frames. Although this method can be considered the fourth method for establishing quantities for calculating semi-rigid frames, it has not yet established a geometric stiffness matrix for semi-rigid beam-column elements, so it cannot be used in second-order analysis.

Thus, for second-order analysis of semi-rigid steel frames, the first method needs to add the geometric stiffness matrix of the beam-column element with both FR ends. The second method needs to be based on the elastic stiffness matrix and geometric stiffness matrix of the FR double-ended beam-column element. The third method needs to be based on the slope-deflection expression of the FR double-ended beam-column element. All these quantities must have existed before. The fourth method also needs to be based on the bending shape functions of the FR double-end beam element, and it has not yet established the geometric stiffness matrix for the semi-rigid beam-column element, so it cannot be used in second-order analysis. Therefore, to independently and synchronously solve the process of building a second-order analysis method for semi-rigid steel frames using the FEM, it is necessary to establish a displacement function or shape function (interpolation function) for the semi-rigid beam-column element. The methods for setting these functions are presented next.

***Fifth method*:** Chan & Ho (1994) [19] expressed the horizontal displacement function (in the form of a third-order polynomial) of an FR double-end beam element as a function of the axial displacement functions (first-order Lagrangian interpolation function), the horizontal, and the rotational displacements of the beam ends. Next, using the spring assembly method of Lui & Chen (1985) [12], where the rotation angle at the beam ends through the spring assembly method is expressed in terms of the rotation angle at the beam end nodes, the bending stiffness of the beam, and the stiffness of the connection. From there, the displacement function of the semi-rigid beam element is obtained. Researchers who have used this approach include Chan (1994) [20], Chui & Chan (1997) [21], and Chan & Chui (2000) [5].

***Sixth method*:** Suarez et al. (1996) [22] adjusted the rotation angle at the beam end in the formula representing the horizontal displacement function according to third-order Hermitian shape functions and the nodal displacement vector of the FR double-end beam element, transforming and obtaining the displacement function of the semi-rigid beam element. This displacement function is expressed in terms of the third-order Hermitian shape functions of the FR double-end beam element, the stiffness of the element, and the stiffness of the connection. This approach is similar to the rotation angle adjustment in the slope-deflection expression of Chen & Lui (1987) [2], but it is applied to the expression of the horizontal displacement function. Researchers who have used this method include Senkulovic & Salatic (2001) [23], Zohra & Nacer (2002) [24], and Salatic (2019) [25].

***Seventh method*:** Developed in Yugoslavia, according to Zlatkov (2015) [26], this method was pioneered by Milićević (1986) [27]. In this method, the fixity factor of the connection at each semi-rigid beam end is calculated as the ratio between the actual rotation angle of the semi-rigid beam end and the rotation angle of the FR beam end. The classical formulas of the first-order theoretical deformation method are used to calculate the rotation angles between the chord and the tangents of the elastic line due to deformation caused by unit displacements placed at the nodes. This rotation angle expression includes element length, fixity factor, and the moment due to unit displacement (expressed through stiffness, element length, and stability functions according to second-order classical calculation theory) at the beam ends. The horizontal displacement function is chosen as a third-order Hermitian polynomial with four parameters as unknowns. Using the unit displacement method, where one displacement is set equal to a unit value while all the remaining displacements are zero, a system of four equations is established from four boundary conditions to determine the four unknown parameters of the semi-rigid beam element shape function, corresponding to the unit displacement under consideration. This process is repeated sequentially for four displacements, including two linear displacements and two rotational displacements, to obtain four shape functions of the semi-rigid beam element. Researchers using this method include Zlatkov et al. (2011) [28] and Zlatkov et al. (2020) [29]. Similarly, Anh (2002) [30, 31] applied the unit displacement method, the virtual work principle, and the shape function of a beam element with two rigid ends to establish the stiffness matrices of a semi-rigid beam-column element. The established quantities were used in a second-order analysis of semi-rigid frames with nodal rigid zones.

The two methods of establishing displacement functions of Chan & Ho (1994) [19] and Suarez et al. (1996) [22], which basically correspond to the two methods for establishing semi-rigid beam-column elements, are spring assembly (Lui & Chen (1985) [12], Xu (1992) [13]) and rotation angle correction [2]. The method of establishing shape functions of Milićević (1986) [27] is characterized by the fact that the constructed shape functions are quite cumbersome and still depend on the stability function of the beam-column element. Second-order analysis of semi-rigid steel frames is still a new field, attracting many researchers, including Nguyen et al. (2021) [32], Dang et al. (2023) [33], and Souza & Verdade (2024) [34]. Some authors have explored novel research directions. For example, Saadi et al. (2021) [35] established seismic fragility curves to assess the performance of semi-rigid connections in steel frames; Genovese & Sofi (2024) [36] developed an interval stiffness matrix for analyzing steel frames with uncertain semi-rigid connections; and Jough & Soori (2024) [37] investigated the effect of semi-rigid connections in steel frame structures during progressive collapse.

This article presents a novel approach that establishes shape functions for a semi-rigid beam-column element directly from the element's geometric characteristics and the stiffness of its semi-rigid connections. The obtained functional formulas of the semi-rigid beam-column element are pure polynomials with parameters built in a simple, coherent, and easy-to-use manner. The shape functions of semi-rigid beam-column elements are fundamental for calculating quantities for second-order analysis of semi-rigid steel frames according to FEM. The present study contributes to FEM by providing these shape functions. Because the shape function formula is a polynomial, similar to the approach of Przemieniecki (1968) [38] for beam-column elements with two rigid ends, the linear elastic stiffness matrix, geometric stiffness matrix, and equilibrium equation of a semi-rigid beam-column element in a local coordinate system are also derived by applying Castigliano's theorem (Part 1) to the elastic deformation potential energy expression. The equivalent nodal load vector of a semi-rigid beam element is obtained from the same formula as for the equivalent nodal load vector of a beam element with both FR ends according to FEM.

2. Establishing the Semi-rigid Beam-column Element Stiffness Matrix

2.1. Establishing the Shape Function of Semi-Rigid Beam-Column Element

Consider a beam-column element e^{th}, where the connections at the ends A and B are elastic rotational springs, forming a semi-rigid beam-column element. The local coordinate system Oxy has the x-axis coincident with the longitudinal axis of the element, the y-axis perpendicular to the element's longitudinal axis and pointing upward, with the origin of coordinates at end A. The symbols A, I, L, and E represent the cross-sectional area, moment of inertia, length, and elastic modulus of the material, respectively. In the i^{th} loading step, the symbols N_A, Q_A, and M_A represent the longitudinal force (in the x-axis direction), shear force (in the y-axis direction), and bending moment (rotation around the z-axis) at end A, respectively, and similarly for N_B, Q_B, and M_B at end B.

The displacements u_A, v_A, and u_B, v_B represent the axial and horizontal (or vertical) displacements of node A and node B, respectively. The rotational displacements around the z-axis of the frame nodes at A and B are denoted by θ_A and θ_B, while θ_{eA} and θ_{eB} are the rotation angles at the beam ends. The connection rotational angles at node A and B are denoted as θ_{cA} and θ_{cB}, respectively. The rotational stiffnesses of the connections at nodes A and B are denoted by k_A and k_B, respectively.

Figure 1 illustrates the kinematic relationship between displacement, internal force, and deformation of an element with a semi-rigid connection. Assuming the semi-rigid connection has no dimensions and neglecting the effects of axial and shear forces on the connection's operation, the element material is considered linearly elastic, the beam follows the Euler-Bernoulli model, and the connection's moment-rotation relationship can be linear, multi-linear, or non-linear.

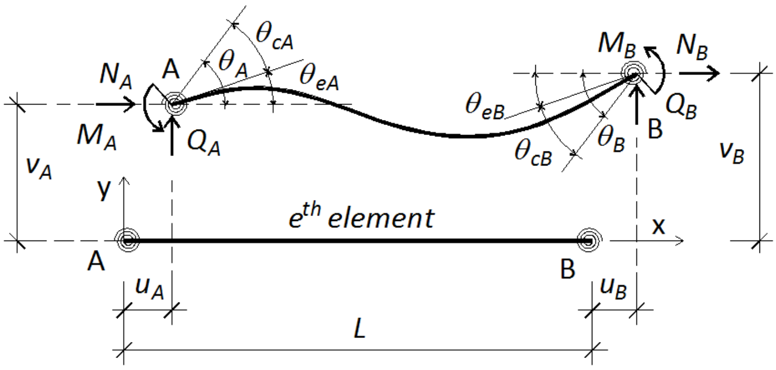

Figure 1. Semi-rigid beam-column element

The nodal displacement vector of the e^{th} element, at the i^{th} loading step, in the local coordinate system is:

$$\{\delta_s\}_e = \{u_A \quad v_A \quad \theta_{eA} \quad u_B \quad v_B \quad \theta_{eB}\}^T \tag{1}$$

To establish the stiffness matrices for the semi-rigid beam-column element, shape functions must be developed considering the stiffness of the connections at both ends. Let the cross-section at position x from end A has three displacement components: axial displacement u_x, horizontal displacement v_x, and rotational displacement θ_x. The rotational and horizontal displacement are related $\theta_x = \frac{dv_x}{dx}$, thus, u_x and v_x are selected as representative displacement functions.

Assuming a polynomial displacement function. For axial load element, each node of the element has one degree of freedom, giving the entire element two degrees of freedom, so the displacement function u_x has two parameters a_1 and a_2. The displacement function polynomial is selected as a first-order form. For bending element, each node has two degrees of freedom, so the displacement function v_x has four parameters a_3, a_4, a_5, and a_6. The displacement function polynomial is chosen as a third-order Hermitian function. The vector of displacement functions is given by:

$$\{u\} = \begin{Bmatrix} u_x \\ v_x \end{Bmatrix} = \begin{Bmatrix} a_1 + a_2 x \\ a_3 + a_4 x + a_5 x^2 + a_6 x^3 \end{Bmatrix} = \begin{bmatrix} 1 & x & 0 & 0 & 0 & 0 \\ 0 & 0 & 1 & x & x^2 & x^3 \end{bmatrix} \{a_1 \quad a_2 \quad a_3 \quad a_4 \quad a_5 \quad a_6\}^T \tag{2}$$

According to the differential relationship, the rotation displacement function can be calculated as follows:

$$\theta_x = v_x^{'} = a_4 + 2a_5x + 3a_6x^2 \tag{3}$$

Combining with the differential equation for deflection, obtaining the moment function M_x:

$$\pm\frac{M_x}{EI} = v_x^{''} = 2a_5 + 6a_6x \tag{4}$$

At end A, $x = 0$:

$$M(x = 0) = M_A = -2EIa_5 \tag{5}$$

At end B, $x = L$:

$$M(x = L) = M_B = 2EIa_5 + 6EILa_6 \tag{6}$$

The rotation angle at nodes A and B can be written as:

$$\begin{aligned} \theta_A &= \theta_{eA} + \theta_{cA} = \theta_{eA} + \frac{M_A}{k_A} \\ \theta_B &= \theta_{eB} + \theta_{cB} = \theta_{eB} + \frac{M_B}{k_B} \end{aligned} \tag{7}$$

Substituting M_A and M_B in Equations 5 and 6 into Equation 7, the expressions for the rotation angles at ends become:

$$\begin{cases} \theta_{eA} = \theta_A + \frac{2EI}{k_A}a_5 \\ \theta_{eB} = \theta_B - \frac{2EI}{k_B}a_5 - \frac{6EIL}{k_B}a_6 \end{cases} \tag{8}$$

Boundary conditions at the ends of the element are then applied:

$$\begin{cases} u_A \equiv u(x = 0) = a_1 \\ v_A \equiv v(x = 0) = a_3 \\ \theta_{eA} \equiv \theta(x = 0) = \theta_A + \frac{2EI}{k_A}a_5 = a_4 \\ u_B \equiv u(x = L) = a_1 + a_2L \\ v_B \equiv v(x = L) = a_3 + a_4L + a_5L^2 + a_6L^3 \\ \theta_{eB} \equiv \theta(x = L) = \theta_B - \frac{2EI}{k_B}a_5 - \frac{6EIL}{k_B}a_6 = a_4 + 2a_5L + 3a_6L^2 \end{cases} \tag{9}$$

Arranging and simplifying Equation 9, it takes the form:

$$\begin{cases} u_A = a_1 \\ v_A = a_3 \\ \theta_A = a_4 - \frac{2EI}{k_A}a_5 \\ u_B = a_1 + a_2L \\ v_B = a_3 + a_4L + a_5L^2 + a_6L^3 \\ \theta_B = a_4 + \frac{2(Lk_B+EI)}{k_B}a_5 + \frac{3(L^2k_B+2EIL)}{k_B}a_6 \end{cases} \tag{10}$$

Write Equation 10 in matrix form:

$$\{\delta_s\}_e = \begin{bmatrix} 1 & 0 & 0 & 0 & 0 & 0 \\ 0 & 0 & 1 & 0 & 0 & 0 \\ 0 & 0 & 0 & 1 & -\frac{2EI}{k_A} & 0 \\ 1 & L & 0 & 0 & 0 & 0 \\ 0 & 0 & 1 & L & L^2 & L^3 \\ 0 & 0 & 0 & 1 & \frac{2(Lk_B+EI)}{k_B} & \frac{3(L^2k_B+2EIL)}{k_B} \end{bmatrix} \begin{Bmatrix} a_1 \\ a_2 \\ a_3 \\ a_4 \\ a_5 \\ a_6 \end{Bmatrix} = [C]\{a\} \tag{11}$$

In Equation 2, we have the symbol:

$$[X(x)] = \begin{bmatrix} 1 & x & 0 & 0 & 0 & 0 \\ 0 & 0 & 1 & x & x^2 & x^3 \end{bmatrix} \tag{12}$$

here $[C]$ is the constant matrix and $[X(x)]$ is a matrix of monomials.

In the FEM, takes the formula:

$$[N(x)] = [X(x)][C]^{-1} = \begin{bmatrix} N_1(x) & 0 & 0 & N_4(x) & 0 & 0 \\ 0 & N_2(x) & N_3(x) & 0 & N_5(x) & N_6(x) \end{bmatrix} \tag{13}$$

Performing the calculation of the inverse matrix $[C]^{-1}$, and substituting Equation 12 into Equation 13, we obtain the shape functional equations as follows:

$$\begin{aligned}
&N_1(x) = 1 - \tfrac{x}{L},\ N_4(x) = \tfrac{x}{L} \\
&N_2(x) = 1 - \tfrac{6xEI(2EI+Lk_B)}{L(12E^2I^2+4EILk_A+4EILk_B+L^2k_Ak_B)} - \tfrac{3x^2(2EI+Lk_B)k_A}{L(12E^2I^2+4EILk_A+4EILk_B+L^2k_Ak_B)} + \tfrac{2x^3(EIk_A+EIk_B+Lk_Ak_B)}{L^2(12E^2I^2+4EILk_A+4EILk_B+L^2k_Ak_B)} \\
&N_3(x) = \tfrac{xL(4EI+Lk_B)k_A}{12E^2I^2+4EILk_A+4EILk_B+L^2k_Ak_B} - \tfrac{2x^2(3EI+Lk_B)k_A}{12E^2I^2+4EILk_A+4EILk_B+L^2k_Ak_B} + \tfrac{x^3(2EI+Lk_B)k_A}{L(12E^2I^2+4EILk_A+4EILk_B+L^2k_Ak_B)} \\
&N_5(x) = \tfrac{6xEI(2EI+Lk_B)}{L(12E^2I^2+4EILk_A+4EILk_B+L^2k_Ak_B)} + \tfrac{3x^2(2EI+Lk_B)k_A}{L(12E^2I^2+4EILk_A+4EILk_B+L^2k_Ak_B)} - \tfrac{2x^3(EIk_A+EIk_B+Lk_Ak_B)}{L^2(12E^2I^2+4EILk_A+4EILk_B+L^2k_Ak_B)} \\
&N_6(x) = -\tfrac{2xLEIk_B}{12E^2I^2+4EILk_A+4EILk_B+L^2k_Ak_B} - \tfrac{x^2Lk_Ak_B}{12E^2I^2+4EILk_A+4EILk_B+L^2k_Ak_B} + \tfrac{x^3(2EI+Lk_A)k_B}{L(12E^2I^2+4EILk_A+4EILk_B+L^2k_Ak_B)}
\end{aligned} \tag{14}$$

In each loading step, the stiffness of connection, length, as well as the geometric characteristics and material properties of the element remain unchanged. The following terms are established for convenience of calculation:

$$\begin{aligned}
&d_0 = 12E^2I^2 + 4EILk_A + 4EILk_B + L^2k_Ak_B,\ d_1 = \tfrac{6EI(2EI+Lk_B)}{Ld_0},\ d_2 = \tfrac{(2EI+Lk_B)k_A}{Ld_0} \\
&d_3 = \tfrac{2(EIk_A+EIk_B+Lk_Ak_B)}{L^2d_0},\ d_4 = \tfrac{L(4EI+Lk_B)k_A}{d_0},\ d_5 = \tfrac{2(3EI+Lk_B)k_A}{d_0},\ d_6 = \tfrac{2LEIk_B}{d_0} \\
&d_7 = \tfrac{Lk_Ak_B}{d_0},\ d_8 = \tfrac{(2EI+Lk_A)k_B}{Ld_0}
\end{aligned} \tag{15}$$

Substituting Equation 15 into Equation 14, formulas of shape function written in shortened form are obtained as follows:

$$\begin{aligned}
&N_1(x) = 1 - \tfrac{x}{L},\ N_2(x) = 1 - d_1x - 3d_2x^2 + d_3x^3,\ N_3(x) = d_4x - d_5x^2 + d_2x^3,\ N_4(x) = \tfrac{x}{L} \\
&N_5(x) = d_1x + 3d_2x^2 - d_3x^3,\ N_6(x) = -d_6x - d_7x^2 + d_8x^3
\end{aligned} \tag{16}$$

In Equation 16, the shape functions of the axial displacement $N_1(x)$ and $N_4(x)$ are linear Lagrangian functions as for normal tension or compression element; and the shape functions of the horizontal displacement $N_2(x)$, $N_3(x)$, $N_5(x)$, and $N_6(x)$ have a similar form to the third-order Hermitian shape functions of a bending element with both FR ends, but there are differences due to the semi-rigid connection at the two ends.

2.2. Method for Establishing Stiffness Matrix and Equilibrium Equation of Semi-Rigid Beam-Column Element

The stiffness matrix of a semi-rigid beam-column element, including both the linear elastic stiffness matrix and the geometric stiffness matrix, is established from the deformation potential energy expression of the semi-rigid beam-column element $U_{s,e}$. Using the Green strain tensor in the Lagrangian coordinate system, and ignoring the influence of shear deformation, the axial principal deformation combination ε_{xx} (including principal deformation due to bending) is expressed as follows:

$$\varepsilon_{xx} = \frac{\partial u_x}{\partial x} - \frac{\partial^2 v_x}{\partial x^2}y + \frac{1}{2}\left(\frac{\partial v_x}{\partial x}\right)^2 \tag{17}$$

Substituting Equation 17 into the expression for the deformation potential energy of the element, expanding and ignoring higher-order terms, obtaining the following formula:

$$U_{s,e} = \frac{EA}{2}\int_0^L \left(\frac{\partial u_x}{\partial x}\right)^2 dx + \frac{EI}{2}\int_0^L \left(\frac{\partial^2 v_x}{\partial x^2}\right)^2 dx + \frac{1}{2}(k_A\theta_{cA}^2 + k_B\theta_{cB}^2) + \frac{EA}{2}\int_0^L \frac{\partial u_x}{\partial x}\left(\frac{\partial v_x}{\partial x}\right)^2 dx \tag{18}$$

Here, the first two terms in formula 18 represent the linear elastic deformation potential energy of the element itself, while the third term represents the linear elastic deformation potential energy at the connection at both ends of element, and the fourth term contributes to the nonlinear strain potential energy of the element.

The linear elastic stiffness matrix is established from the linear elastic deformation potential of the element itself:

$$U_{Es,e} = \frac{EA}{2}\int_0^L \left(\frac{\partial u_x}{\partial x}\right)^2 dx + \frac{EI}{2}\int_0^L \left(\frac{\partial^2 v_x}{\partial x^2}\right)^2 dx \tag{19}$$

and from the linear elastic deformation potential energy of the connections at ends A and B:

$$U_{Cs,e} = \frac{1}{2}k_A\theta_{cA}^2 + \frac{1}{2}k_B\theta_{cB}^2 \quad (20)$$

The geometric stiffness matrix is established from the nonlinear deformation potential energy of the element:

$$U_{P-Ds,e} = \frac{EA}{2}\int_0^L \frac{\partial u_x}{\partial x}\left(\frac{\partial v_x}{\partial x}\right)^2 dx \quad (21)$$

Equation 18 is written as:

$$U_{s,e} = U_{Es,e} + U_{Cs,e} + U_{P-Ds,e} = U_{L-Es,e} + U_{P-Ds,e} \quad (22)$$

wherein:

$$U_{L-Es,e} = U_{Es,e} + U_{Cs,e} \quad (23)$$

Equation 23 represents the linear elastic deformation potential energy of the element, including the elastic potential energy of the element itself, and the elastic potential energy of the connections.

Let $\{P_s\}_e$ be the nodal load vector in the local coordinate system, $[k_{L-Es}]_e$ be the linear elastic stiffness matrix, and $[k_{Gs}]_e$ be the geometric stiffness matrix of semi-rigid beam-column element. By applying Castigliano's theorem (Part 1), obtaining the relationship between load, deformation potential energy, and displacement of e^{th} element:

$$\{P_s\}_e = \frac{\partial U_{s,e}}{\partial \delta_s} = ([k_{L-Es}]_e + [k_{Gs}]_e)\{\delta_s\}_e = [k_s]_e\{\delta_s\}_e \quad (24)$$

Or in shortened form, having the equilibrium equation of the e^{th} element in the local coordinate system:

$$\{P_s\}_e = [k_s]_e\{\delta_s\}_e \quad (25)$$

Here,

$$[k_s]_e = [k_{L-Es}]_e + [k_{Gs}]_e \quad (26)$$

represents stiffness matrix of the element with two semi-rigid connection ends, there:

$$[k_{L-Es}]_e = [k_{Es}]_e + [k_{Cs}]_e \quad (27)$$

with $[k_{Es}]_e$ and $[k_{Cs}]_e$ are the linear elastic stiffness matrix of the element itself and the linear elastic stiffness matrix of the connections, respectively.

In FEM, the distribution of displacements in the element is represented through the shape function and nodal displacement vector as follows:

$$\{u_x \quad v_x\}^T = [N(x)]\{\delta_s\}_e \quad (28)$$

Substituting the shape functions from formula 16 into 28, the nodal displacement vector takes the form:

$$\begin{Bmatrix} u_x \\ v_x \end{Bmatrix} = \begin{bmatrix} 1-\frac{x}{L} & 0 & 0 & \frac{x}{L} & 0 & 0 \\ 0 & 1-d_1x-3d_2x^2+d_3x^3 & d_4x-d_5x^2+d_2x^3 & 0 & d_1x+3d_2x^2-d_3x^3 & -d_6x-d_7x^2+d_8x^3 \end{bmatrix} \times \{u_A \quad v_A \quad \theta_{eA} \quad u_B \quad v_B \quad \theta_{eB}\}^T \quad (29)$$

Expanding and calculating the partial derivatives in Equation 29, obtaining the following expressions:

$$\frac{\partial u_x}{\partial x} = \frac{1}{L}(-u_A + u_B) \quad (30)$$

$$\frac{\partial v_x}{\partial x} = (-d_1 - 6d_2x + 3d_3x^2)v_A + (d_4 - 2d_5x + 3d_2x^2)\theta_{eA} + (d_1 + 6d_2x - 3d_3x^2)v_B + (-d_6 - 2d_7x + 3d_8x^2)\theta_{eB} \quad (31)$$

$$\frac{\partial^2 v_x}{\partial x^2} = (-6d_2 + 6d_3x)v_A + (-2d_5 + 6d_2x)\theta_{eA} + (6d_2 - 6d_3x)v_B + (-2d_7 + 6d_8x)\theta_{eB} \quad (32)$$

The stiffness matrices are further elaborated in the next section.

2.3. Establishing the Linear Elastic Stiffness Matrix Formula

The linear elastic stiffness matrix is determined by the formula:

$$\frac{\partial U_{L-Es,e}}{\partial \delta_s} = [k_{L-Es}]_e\{\delta_s\}_e = ([k_{Es}]_e + [k_{Cs}]_e)\{\delta_s\}_e = [k_{Es}]_e\{\delta_s\}_e + [k_{Cs}]_e\{\delta_s\}_e \quad (33)$$

Or in expanded form for the linear elastic stiffness matrix of the element itself:

$$\left\{\frac{\partial U_{Es,e}}{\partial u_A} \quad \frac{\partial U_{Es,e}}{\partial v_A} \quad \frac{\partial U_{Es,e}}{\partial \theta_{eA}} \quad \frac{\partial U_{Es,e}}{\partial u_B} \quad \frac{\partial U_{Es,e}}{\partial v_B} \quad \frac{\partial U_{Es,e}}{\partial \theta_{eB}}\right\}^T = [k_{Es}]_e\{\delta_s\}_e \tag{34}$$

And similarly for the linear elastic stiffness matrix of the connections:

$$\left\{\frac{\partial U_{Cs,e}}{\partial u_A} \quad \frac{\partial U_{Cs,e}}{\partial v_A} \quad \frac{\partial U_{Cs,e}}{\partial \theta_{eA}} \quad \frac{\partial U_{Cs,e}}{\partial u_B} \quad \frac{\partial U_{Cs,e}}{\partial v_B} \quad \frac{\partial U_{Cs,e}}{\partial \theta_{eB}}\right\}^T = [k_{Cs}]_e\{\delta_s\}_e \tag{35}$$

To calculate the elastic deformation potential energy of the element itself, substitute Equations 30 and 32 into 19, and integral, obtaining the following expressions:

$$U_{Es,e} = \frac{EA}{2L}(u_A^2 - 2u_Au_B + u_B^2) + \frac{EI}{2}\begin{bmatrix} (36d_2^2L - 36d_2d_3L^2 + 12d_3^2L^3)v_A^2 + (12d_2^2L^3 - 12d_2d_5L^2 + 4d_5^2L)\theta_{eA}^2 \\ +(36d_2^2L - 36d_2d_3L^2 + 12d_3^2L^3)v_B^2 \\ +(4d_7^2L - 12d_7d_8L^2 + 12d_8^2L^3)\theta_{eB}^2 \\ +(-36d_2^2L^2 + 24d_2d_3L^3 + 24d_2d_5L - 12d_3d_5L^2)v_A\theta_{eA} \\ +(-72d_2^2L + 72d_2d_3L^2 - 24d_3^2L^3)v_Av_B \\ +(24d_2d_7L - 36d_2d_8L^2 - 12d_3d_7L^2 + 24d_3d_8L^3)v_A\theta_{eB} \\ +(36d_2^2L^2 - 24d_2d_3L^3 - 24d_2d_5L + 12d_3d_5L^2)\theta_{eA}v_B \\ +(-12d_2d_7L^2 + 24d_2d_8L^3 + 8d_5d_7L - 12d_5d_8L^2)\theta_{eA}\theta_{eB} \\ +(-24d_2d_7L + 36d_2d_8L^2 + 12d_3d_7L^2 - 24d_3d_8L^3)v_B\theta_{eB} \end{bmatrix} \tag{36}$$

Next, calculating the elastic deformation potential energy in the connection according to Equation 20.

From Equation 32, at $x = 0$

$$M_A = -EI\frac{\partial^2 v_x}{\partial x^2} = 6EId_2v_A + 2EId_5\theta_{eA} - 6EId_2v_B + 2EId_7\theta_{eB} \tag{37}$$

The moment and rotation angle in the connection at end A are determined by the formula:

$$M_A = k_A\theta_{cA} \tag{38}$$

Substituting Equation 38 into Equation 37, the rotation angle in the connection at end A can be calculated as:

$$\theta_{cA} = \frac{2EI}{k_A}(3d_2v_A + d_5\theta_{eA} - 3d_2v_B + d_7\theta_{eB}) \tag{39}$$

From Equation 32, at $x = L$:

$$M_B = EI\frac{\partial^2 v_x}{\partial x^2} = EI[(-6d_2 + 6d_3L)v_A + (-2d_5 + 6d_2L)\theta_{eA} + (6d_2 - 6d_3L)v_B + (-2d_7 + 6d_8L)\theta_{eB}] \tag{40}$$

The moment and rotation angle in the connection at end B are determined by the formula:

$$M_B = k_B\theta_{cB} \tag{41}$$

Substituting Equation 41 into Equation 40, the rotation angle in the connection at end B can be calculated as:

$$\theta_{cB} = \frac{EI}{k_B}[(-6d_2 + 6d_3L)v_A + (-2d_5 + 6d_2L)\theta_{eA} + (6d_2 - 6d_3L)v_B + (-2d_7 + 6d_8L)\theta_{eB}] \tag{42}$$

Simplify the displacement coefficients in Equation 42, and determine:

$$d_9 = \frac{2(3EI + Lk_A)k_B}{d_0} \tag{43}$$

Substituting Equation 43 into Equation 42, getting the rotation angle formula in the connection at end B:

$$\theta_{cB} = \frac{2EI}{k_B}(3d_8v_A + d_7\theta_{eA} - 3d_8v_B + d_9\theta_{eB}) \tag{44}$$

Substituting Equations 39 and 44 into Equation 20, expanding and grouping according to each type of transposition:

$$U_{Cs,e} = 2E^2I^2\left[\frac{1}{k_A}(3d_2v_A + d_5\theta_{eA} - 3d_2v_B + d_7\theta_{eB})^2 + \frac{1}{k_B}(3d_8v_A + d_7\theta_{eA} - 3d_8v_B + d_9\theta_{eB})^2\right] \tag{45}$$

Expanding Equation 45, obtaining the following expressions:

$$U_{Cs,e}=2E^2I^2\begin{bmatrix}\left(\frac{9d_2^2}{k_A}+\frac{9d_8^2}{k_B}\right)v_A^2+\left(\frac{d_5^2}{k_A}+\frac{d_7^2}{k_B}\right)\theta_{eA}^2+\left(\frac{9d_2^2}{k_A}+\frac{9d_8^2}{k_B}\right)v_B^2+\left(\frac{d_7^2}{k_A}+\frac{d_9^2}{k_B}\right)\theta_{eB}^2\\+\left(\frac{6d_2d_5}{k_A}+\frac{6d_7d_8}{k_B}\right)v_A\theta_{eA}-\left(\frac{18d_2^2}{k_A}+\frac{18d_8^2}{k_B}\right)v_Av_B+\left(\frac{6d_2d_7}{k_A}+\frac{6d_8d_9}{k_B}\right)v_A\theta_{eB}\\-\left(\frac{6d_2d_5}{k_A}+\frac{6d_7d_8}{k_B}\right)\theta_{eA}v_B+\left(\frac{2d_5d_7}{k_A}+\frac{2d_7d_9}{k_B}\right)\theta_{eA}\theta_{eB}-\left(\frac{6d_2d_7}{k_A}+\frac{6d_8d_9}{k_B}\right)v_B\theta_{eB}\end{bmatrix} \tag{46}$$

The linear elastic stiffness matrix of the semi-rigid beam-column element itself is obtained by substituting Equation 36 into Equation 34:

$$[k_{Es}]_e=\begin{bmatrix}k_{Es}^{1,1}&0&0&k_{Es}^{1,4}&0&0\\0&k_{Es}^{2,2}&k_{Es}^{2,3}&0&k_{Es}^{2,5}&k_{Es}^{2,6}\\0&k_{Es}^{3,2}&k_{Es}^{3,3}&0&k_{Es}^{3,5}&k_{Es}^{3,6}\\k_{Es}^{4,1}&0&0&k_{Es}^{4,4}&0&0\\0&k_{Es}^{5,2}&k_{Es}^{5,3}&0&k_{Es}^{5,5}&k_{Es}^{5,6}\\0&k_{Es}^{6,2}&k_{Es}^{6,3}&0&k_{Es}^{6,5}&k_{Es}^{6,6}\end{bmatrix} \tag{47}$$

wherein:

$k_{Es}^{1,1}=\frac{EA}{L}$, $k_{Es}^{1,4}=k_{Es}^{4,1}=-\frac{EA}{L}$, $k_{Es}^{4,4}=\frac{EA}{L}$, $k_{Es}^{2,2}=12EI(3d_2^2L-3d_2d_3L^2+d_3^2L^3)$

$k_{Es}^{2,3}=k_{Es}^{3,2}=6EI(-3d_2^2L^2+2d_2d_3L^3+2d_2d_5L-d_3d_5L^2)$, $k_{Es}^{2,5}=k_{Es}^{5,2}=-12EI(3d_2^2L-3d_2d_3L^2+d_3^2L^3)$

$k_{Es}^{2,6}=k_{Es}^{6,2}=6EI(2d_2d_7L-3d_2d_8L^2-d_3d_7L^2+2d_3d_8L^3)$, $k_{Es}^{3,3}=4EI(3d_2^2L^3-3d_2d_5L^2+d_5^2L)$

$k_{Es}^{3,5}=k_{Es}^{5,3}=-6EI(-3d_2^2L^2+2d_2d_3L^3+2d_2d_5L-d_3d_5L^2)$

$k_{Es}^{3,6}=k_{Es}^{6,3}=2EI(-3d_2d_7L^2+6d_2d_8L^3+2d_5d_7L-3d_5d_8L^2)$, $k_{Es}^{5,5}=12EI(3d_2^2L-3d_2d_3L^2+d_3^2L^3)$

$k_{Es}^{5,6}=k_{Es}^{6,5}=-6EI(2d_2d_7L-3d_2d_8L^2-d_3d_7L^2+2d_3d_8L^3)$, $k_{Es}^{6,6}=4EI(d_7^2L-3d_7d_8L^2+3d_8^2L^3)$

The linear elastic stiffness matrix of the semi-rigid connection at both ends of element eth is obtained by substituting Equation 46 into Equation 35:

$$[k_{Cs}]_e=\begin{bmatrix}0&0&0&0&0&0\\0&k_{Cs}^{2,2}&k_{Cs}^{2,3}&0&k_{Cs}^{2,5}&k_{Cs}^{2,6}\\0&k_{Cs}^{3,2}&k_{Cs}^{3,3}&0&k_{Cs}^{3,5}&k_{Cs}^{3,6}\\0&0&0&0&0&0\\0&k_{Cs}^{5,2}&k_{Cs}^{5,3}&0&k_{Cs}^{5,5}&k_{Cs}^{5,6}\\0&k_{Cs}^{6,2}&k_{Cs}^{6,3}&0&k_{Cs}^{6,5}&k_{Cs}^{6,6}\end{bmatrix} \tag{48}$$

wherein:

$k_{Cs}^{2,2}=36E^2I^2\left(\frac{d_2^2}{k_A}+\frac{d_8^2}{k_B}\right)$

$k_{Cs}^{2,3}=k_{Cs}^{3,2}=12E^2I^2\left(\frac{d_2d_5}{k_A}+\frac{d_7d_8}{k_B}\right)$

$k_{Cs}^{2,5}=k_{Cs}^{5,2}=-36E^2I^2\left(\frac{d_2^2}{k_A}+\frac{d_8^2}{k_B}\right)$

$k_{Cs}^{2,6}=k_{Cs}^{6,2}=12E^2I^2\left(\frac{d_2d_7}{k_A}+\frac{d_8d_9}{k_B}\right)$

$k_{Cs}^{3,3}=4E^2I^2\left(\frac{d_5^2}{k_A}+\frac{d_7^2}{k_B}\right)$

$k_{Cs}^{3,5}=k_{Cs}^{5,3}=-12E^2I^2\left(\frac{d_2d_5}{k_A}+\frac{d_7d_8}{k_B}\right)$

$k_{Cs}^{3,6}=k_{Cs}^{6,3}=4E^2I^2\left(\frac{d_5d_7}{k_A}+\frac{d_7d_9}{k_B}\right)$

$k_{Cs}^{5,5}=36E^2I^2\left(\frac{d_2^2}{k_A}+\frac{d_8^2}{k_B}\right)$

$k_{Cs}^{5,6}=k_{Cs}^{6,5}=-12E^2I^2\left(\frac{d_2d_7}{k_A}+\frac{d_8d_9}{k_B}\right)$

$k_{Cs}^{6,6}=4E^2I^2\left(\frac{d_7^2}{k_A}+\frac{d_9^2}{k_B}\right)$

The coefficients of the elastic stiffness matrix $[k_{L-Es}]_e$ in Equation 27 have the form:

$$[k_{L-Es}]_e=\begin{bmatrix} k_{L-Es}^{1,1} & 0 & 0 & k_{L-Es}^{1,4} & 0 & 0 \\ 0 & k_{L-Es}^{2,2} & k_{L-Es}^{2,3} & 0 & k_{L-Es}^{2,5} & k_{L-Es}^{2,6} \\ 0 & k_{L-Es}^{3,2} & k_{L-Es}^{3,3} & 0 & k_{L-Es}^{3,5} & k_{L-Es}^{3,6} \\ k_{L-Es}^{4,1} & 0 & 0 & k_{L-Es}^{4,4} & 0 & 0 \\ 0 & k_{L-Es}^{5,2} & k_{L-Es}^{5,3} & 0 & k_{L-Es}^{5,5} & k_{L-Es}^{5,6} \\ 0 & k_{L-Es}^{6,2} & k_{L-Es}^{6,3} & 0 & k_{L-Es}^{6,5} & k_{L-Es}^{6,6} \end{bmatrix} \tag{49}$$

wherein: $k_{L-Es}^{\eta,\kappa}=k_{Es}^{\eta,\kappa}+k_{Cs}^{\eta,\kappa}$, with $\eta=1\div 6$ and $\kappa=1\div 6$.

A special case of the linear elastic stiffness matrix of a semi-rigid beam-column element is when the semi-rigid connections are pin (stiffness approaching zero), or FR (fully rigid, stiffness approaching infinity). Thus, there are four special cases, including: both ends are FR connections; one end is FR, and the other is a pin connection; one end is a pin connection, and the other is a FR connection; or both ends are pin connections. To calculate the special cases, the limits of the matrix terms in Equation 49 need to be determined. The calculation results are given in Table 1.

Table 1. Terms of the linear elastic stiffness matrix of semi-rigid beam-column element in special cases

Matrix term $[k_{L-Es}]_e$	**Both ends FR** $k_A\to\infty, k_B\to\infty$	**End A FR, end B pin** $k_A\to\infty, k_B\to 0$	**End A pin, end B FR** $k_A\to 0, k_B\to\infty$	**Both ends pin** $k_A\to 0, k_B\to 0$
$k_{L-Es}^{2,2}$	$\frac{12EI}{L^3}$	$\frac{3EI}{L^3}$	$\frac{3EI}{L^3}$	0
$k_{L-Es}^{2,3}, k_{L-Es}^{3,2}$	$\frac{6EI}{L^2}$	$\frac{3EI}{L^2}$	0	0
$k_{L-Es}^{2,5}, k_{L-Es}^{5,2}$	$-\frac{12EI}{L^3}$	$-\frac{3EI}{L^3}$	$-\frac{3EI}{L^3}$	0
$k_{L-Es}^{2,6}, k_{L-Es}^{6,2}$	$\frac{6EI}{L^2}$	0	$\frac{3EI}{L^2}$	0
$k_{L-Es}^{3,3}$	$\frac{4EI}{L}$	$\frac{3EI}{L}$	0	0
$k_{L-Es}^{3,5}, k_{L-Es}^{5,3}$	$-\frac{6EI}{L^2}$	$-\frac{3EI}{L^2}$	0	0
$k_{L-Es}^{3,6}, k_{L-Es}^{6,3}$	$\frac{2EI}{L}$	0	0	0
$k_{L-Es}^{5,5}$	$\frac{12EI}{L^3}$	$\frac{3EI}{L^3}$	$\frac{3EI}{L^3}$	0
$k_{L-Es}^{5,6}, k_{L-Es}^{6,5}$	$-\frac{6EI}{L^2}$	0	$-\frac{3EI}{L^2}$	0
$k_{L-Es}^{6,6}$	$\frac{4EI}{L}$	0	$\frac{3EI}{L}$	0

Compiling Table 1 into a matrix, for each special case, as follows:

- Element with both ends are FR connections:

$$[k_{L-Es}]_e=\begin{bmatrix} \frac{EA}{L} & 0 & 0 & -\frac{EA}{L} & 0 & 0 \\ 0 & \frac{12EI}{L^3} & \frac{6EI}{L^2} & 0 & -\frac{12EI}{L^3} & \frac{6EI}{L^2} \\ 0 & \frac{6EI}{L^2} & \frac{4EI}{L} & 0 & -\frac{6EI}{L^2} & \frac{2EI}{L} \\ -\frac{EA}{L} & 0 & 0 & \frac{EA}{L} & 0 & 0 \\ 0 & -\frac{12EI}{L^3} & -\frac{6EI}{L^2} & 0 & \frac{12EI}{L^3} & -\frac{6EI}{L^2} \\ 0 & \frac{6EI}{L^2} & \frac{2EI}{L} & 0 & -\frac{6EI}{L^2} & \frac{4EI}{L} \end{bmatrix} \tag{50}$$

- Element with end A is FR connection, and end B is pin connection:

$$[k_{L-Es}]_e=\begin{bmatrix} \frac{EA}{L} & 0 & 0 & -\frac{EA}{L} & 0 & 0 \\ 0 & \frac{3EI}{L^3} & \frac{3EI}{L^2} & 0 & -\frac{3EI}{L^3} & 0 \\ 0 & \frac{3EI}{L^2} & \frac{3EI}{L} & 0 & -\frac{3EI}{L^2} & 0 \\ -\frac{EA}{L} & 0 & 0 & \frac{EA}{L} & 0 & 0 \\ 0 & -\frac{3EI}{L^3} & -\frac{3EI}{L^2} & 0 & \frac{3EI}{L^3} & 0 \\ 0 & 0 & 0 & 0 & 0 & 0 \end{bmatrix} \tag{51}$$

- Element with end A is pin connection, and end B is FR connection:

$$[k_{L-Es}]_e = \begin{bmatrix} \frac{EA}{L} & 0 & 0 & -\frac{EA}{L} & 0 & 0 \\ 0 & \frac{3EI}{L^3} & 0 & 0 & -\frac{3EI}{L^3} & \frac{3EI}{L^2} \\ 0 & 0 & 0 & 0 & 0 & 0 \\ -\frac{EA}{L} & 0 & 0 & \frac{EA}{L} & 0 & 0 \\ 0 & -\frac{3EI}{L^3} & 0 & 0 & \frac{3EI}{L^3} & -\frac{3EI}{L^2} \\ 0 & \frac{3EI}{L^2} & 0 & 0 & -\frac{3EI}{L^2} & \frac{3EI}{L} \end{bmatrix} \tag{52}$$

- Element with both ends are pin connections:

$$[k_{L-Es}]_e = \begin{bmatrix} \frac{EA}{L} & 0 & 0 & -\frac{EA}{L} & 0 & 0 \\ 0 & 0 & 0 & 0 & 0 & 0 \\ 0 & 0 & 0 & 0 & 0 & 0 \\ -\frac{EA}{L} & 0 & 0 & \frac{EA}{L} & 0 & 0 \\ 0 & 0 & 0 & 0 & 0 & 0 \\ 0 & 0 & 0 & 0 & 0 & 0 \end{bmatrix} \tag{53}$$

These established special cases are correspondingly equal to the linear elastic stiffness matrices of element whose connections at the ends are FR or pin, in FEM.

2.4. Establishing the Geometric Stiffness Matrix Formula

The linear elastic stiffness matrix is determined by the formula:

$$\frac{\partial U_{P-Ds,e}}{\partial \delta_s} = [k_{Gs}]_e \{\delta_s\}_e \tag{54}$$

Or, in an expanded form:

$$\left\{ \frac{\partial U_{P-Ds,e}}{\partial u_A} \quad \frac{\partial U_{P-Ds,e}}{\partial v_A} \quad \frac{\partial U_{P-Ds,e}}{\partial \theta_{eA}} \quad \frac{\partial U_{P-Ds,e}}{\partial u_B} \quad \frac{\partial U_{P-Ds,e}}{\partial v_B} \quad \frac{\partial U_{P-Ds,e}}{\partial \theta_{eB}} \right\}^T = [k_{Gs}]_e \{\delta_s\}_e \tag{55}$$

Substitute Equations 30 and 31 into Equation 21 and integrate

$$U_{P-Ds,e} = \frac{EA}{2L}(u_B - u_A) \begin{bmatrix} +\left(d_1^2L + 6d_1d_2L^2 - 2d_1d_3L^3 + 12d_2^2L^3 - 9d_2d_3L^4 + \frac{9}{5}d_3^2L^5\right)v_A^2 \\ +\left(\frac{9}{5}d_2^2L^5 + 2d_2d_4L^3 - 3d_2d_5L^4 + d_4^2L - 2d_4d_5L^2 + \frac{4}{3}d_5^2L^3\right)\theta_{eA}^2 \\ +\left(d_1^2L + 6d_1d_2L^2 - 2d_1d_3L^3 + 12d_2^2L^3 - 9d_2d_3L^4 + \frac{9}{5}d_3^2L^5\right)v_B^2 \\ +\left(d_6^2L + 2d_6d_7L^2 - 2d_6d_8L^3 + \frac{4}{3}d_7^2L^3 - 3d_7d_8L^4 + \frac{9}{5}d_8^2L^5\right)\theta_{eB}^2 \\ +\left(-2d_1d_2L^3 - 2d_1d_4L + 2d_1d_5L^2 - 9d_2^2L^4 + \frac{18}{5}d_2d_3L^5 - 6d_2d_4L^2 + 8d_2d_5L^3 + 2d_3d_4L^3 - 3d_3d_5L^4\right)v_A\theta_{eA} \\ +\left(-2d_1^2L - 12d_1d_2L^2 + 4d_1d_3L^3 - 24d_2^2L^3 + 18d_2d_3L^4 - \frac{18}{5}d_3^2L^5\right)v_Av_B \\ +\left(2d_1d_6L + 2d_1d_7L^2 - 2d_1d_8L^3 + 6d_2d_6L^2 + 8d_2d_7L^3 - 9d_2d_8L^4 - 2d_3d_6L^3 - 3d_3d_7L^4 + \frac{18}{5}d_3d_8L^5\right)v_A\theta_{eB} \\ +\left(2d_1d_2L^3 + 2d_1d_4L - 2d_1d_5L^2 + 9d_2^2L^4 - \frac{18}{5}d_2d_3L^5 + 6d_2d_4L^2 - 8d_2d_5L^3 - 2d_3d_4L^3 + 3d_3d_5L^4\right)\theta_{eA}v_B \\ +\left(-2d_2d_6L^3 - 3d_2d_7L^4 + \frac{18}{5}d_2d_8L^5 + 2d_4d_6L - 2d_4d_7L^2 + 2d_4d_8L^3 + 2d_5d_6L^2 + \frac{8}{3}d_5d_7L^3 - 3d_5d_8L^4\right)\theta_{eA}\theta_{eB} \\ +\left(-2d_1d_6L - 2d_1d_7L^2 + 2d_1d_8L^3 - 6d_2d_6L^2 - 8d_2d_7L^3 + 9d_2d_8L^4 + 2d_3d_6L^3 + 3d_3d_7L^4 - \frac{18}{5}d_3d_8L^5\right)v_B\theta_{eB} \end{bmatrix} \tag{56}$$

to determine the nonlinear deformation potential energy.

In calculating the geometric stiffness matrix, consider the axial force in the element to be constant, and have the following value:

$$N = \frac{EA}{L}(u_B - u_A) \tag{57}$$

The geometric stiffness matrix of the semi-rigid beam-column element is obtained by substituting Equation 57 into Equation 56, and continue substituting into Equation 55:

$$[k_{Gs}]_e = N \begin{bmatrix} 0 & 0 & 0 & 0 & 0 & 0 \\ 0 & k_{Gs}^{2,2} & k_{Gs}^{2,3} & 0 & k_{Gs}^{2,5} & k_{Gs}^{2,6} \\ 0 & k_{Gs}^{3,2} & k_{Gs}^{3,3} & 0 & k_{Gs}^{3,5} & k_{Gs}^{3,6} \\ 0 & 0 & 0 & 0 & 0 & 0 \\ 0 & k_{Gs}^{5,2} & k_{Gs}^{5,3} & 0 & k_{Gs}^{5,5} & k_{Gs}^{5,6} \\ 0 & k_{Gs}^{6,2} & k_{Gs}^{6,3} & 0 & k_{Gs}^{6,5} & k_{Gs}^{6,6} \end{bmatrix} \tag{58}$$

wherein:

$$k_{Gs}^{2,2} = d_1^2 L + 6d_1 d_2 L^2 - 2d_1 d_3 L^3 + 12 d_2^2 L^3 - 9 d_2 d_3 L^4 + \tfrac{9}{5} d_3^2 L^5$$

$$k_{Gs}^{2,3} = k_{Gs}^{3,2} = \left(-d_1 d_2 L^3 - d_1 d_4 L + d_1 d_5 L^2 - \tfrac{9}{2} d_2^2 L^4 + \tfrac{9}{5} d_2 d_3 L^5 - 3 d_2 d_4 L^2 + 4 d_2 d_5 L^3 + d_3 d_4 L^3 - \tfrac{3}{2} d_3 d_5 L^4\right)$$

$$k_{Gs}^{2,5} = k_{Gs}^{5,2} = -d_1^2 L - 6 d_1 d_2 L^2 + 2 d_1 d_3 L^3 - 12 d_2^2 L^3 + 9 d_2 d_3 L^4 - \tfrac{9}{5} d_3^2 L^5$$

$$k_{Gs}^{2,6} = k_{Gs}^{6,2} = \left(d_1 d_6 L + d_1 d_7 L^2 - d_1 d_8 L^3 + 3 d_2 d_6 L^2 + 4 d_2 d_7 L^3 - \tfrac{9}{2} d_2 d_8 L^4 - d_3 d_6 L^3 - \tfrac{3}{2} d_3 d_7 L^4 + \tfrac{9}{5} d_3 d_8 L^5\right)$$

$$k_{Gs}^{3,3} = \tfrac{9}{5} d_2^2 L^5 + 2 d_2 d_4 L^3 - 3 d_2 d_5 L^4 + d_4^2 L - 2 d_4 d_5 L^2 + \tfrac{4}{3} d_5^2 L^3$$

$$k_{Gs}^{3,5} = k_{Gs}^{5,3} = \left(d_1 d_2 L^3 + d_1 d_4 L - d_1 d_5 L^2 + \tfrac{9}{2} d_2^2 L^4 - \tfrac{9}{5} d_2 d_3 L^5 + 3 d_2 d_4 L^2 - 4 d_2 d_5 L^3 - d_3 d_4 L^3 + \tfrac{3}{2} d_3 d_5 L^4\right)$$

$$k_{Gs}^{3,6} = k_{Gs}^{6,3} = \left(-d_2 d_6 L^3 - \tfrac{3}{2} d_2 d_7 L^4 + \tfrac{9}{5} d_2 d_8 L^5 + d_4 d_6 L - d_4 d_7 L^2 + d_4 d_8 L^3 + d_5 d_6 L^2 + \tfrac{4}{3} d_5 d_7 L^3 - \tfrac{3}{2} d_5 d_8 L^4\right)$$

$$k_{Gs}^{5,5} = d_1^2 L + 6 d_1 d_2 L^2 - 2 d_1 d_3 L^3 + 12 d_2^2 L^3 - 9 d_2 d_3 L^4 + \tfrac{9}{5} d_3^2 L^5$$

$$k_{Gs}^{5,6} = k_{Gs}^{6,5} = \left(-d_1 d_6 L - d_1 d_7 L^2 + d_1 d_8 L^3 - 3 d_2 d_6 L^2 - 4 d_2 d_7 L^3 + \tfrac{9}{2} d_2 d_8 L^4 + d_3 d_6 L^3 + \tfrac{3}{2} d_3 d_7 L^4 - \tfrac{9}{5} d_3 d_8 L^5\right)$$

$$k_{Gs}^{6,6} = d_6^2 L + 2 d_6 d_7 L^2 - 2 d_6 d_8 L^3 + \tfrac{4}{3} d_7^2 L^3 - 3 d_7 d_8 L^4 + \tfrac{9}{5} d_8^2 L^5$$

Similarly, the linear elastic stiffness matrix, special cases of the geometric stiffness matrix are obtained by finding the limits of the matrix terms in Equation 58. The calculation results are in Table 2 as follows:

Table 2. Terms of the geometric stiffness matrix of semi-rigid beam-column element in a particular case

Matrix term $[k_{Gs}]_e$	**Both ends FR** $k_A \to \infty, k_B \to \infty$	**End A FR, end B pin** $k_A \to \infty, k_B \to 0$	**End A pin, End B FR** $k_A \to 0, k_B \to \infty$	**Both ends pin** $k_A \to 0, k_B \to 0$
$k_{Gs}^{2,2}$	$\frac{6}{5L}$	$\frac{6}{5L}$	$\frac{6}{5L}$	$\frac{1}{L}$
$k_{Gs}^{2,3}, k_{Gs}^{3,2}$	$\frac{1}{10}$	$\frac{1}{5}$	0	0
$k_{Gs}^{2,5}, k_{Gs}^{5,2}$	$-\frac{6}{5L}$	$-\frac{6}{5L}$	$-\frac{6}{5L}$	$-\frac{1}{L}$
$k_{Gs}^{2,6}, k_{Gs}^{6,2}$	$\frac{1}{10}$	0	$\frac{1}{5}$	0
$k_{Gs}^{3,3}$	$\frac{2L}{15}$	$\frac{L}{5}$	0	0
$k_{Gs}^{3,5}, k_{Gs}^{5,3}$	$-\frac{1}{10}$	$-\frac{1}{5}$	0	0
$k_{Gs}^{3,6}, k_{Gs}^{6,3}$	$-\frac{L}{30}$	0	0	0
$k_{Gs}^{5,5}$	$\frac{6}{5L}$	$\frac{6}{5L}$	$\frac{6}{5L}$	$\frac{1}{L}$
$k_{Gs}^{5,6}, k_{Gs}^{6,5}$	$-\frac{1}{10}$	0	$-\frac{1}{5}$	0
$k_{Gs}^{6,6}$	$\frac{2L}{15}$	0	$\frac{L}{5}$	0

Compiling Table 2 into a matrix, for each special case, as follows:

- Element with both ends are FR connections:

$$[k_{Gs}]_e = N\begin{bmatrix} 0 & 0 & 0 & 0 & 0 & 0 \\ 0 & \frac{6}{5L} & \frac{1}{10} & 0 & -\frac{6}{5L} & \frac{1}{10} \\ 0 & \frac{1}{10} & \frac{2L}{15} & 0 & -\frac{1}{10} & -\frac{L}{30} \\ 0 & 0 & 0 & 0 & 0 & 0 \\ 0 & -\frac{6}{5L} & -\frac{1}{10} & 0 & \frac{6}{5L} & -\frac{1}{10} \\ 0 & \frac{1}{10} & -\frac{L}{30} & 0 & -\frac{1}{10} & \frac{2L}{15} \end{bmatrix} \tag{59}$$

- Element with end A is FR connection, and end B is pin connection:

$$[k_{Gs}]_e = N\begin{bmatrix} 0 & 0 & 0 & 0 & 0 & 0 \\ 0 & \frac{6}{5L} & \frac{1}{5} & 0 & -\frac{6}{5L} & 0 \\ 0 & \frac{1}{5} & \frac{L}{5} & 0 & -\frac{1}{5} & 0 \\ 0 & 0 & 0 & 0 & 0 & 0 \\ 0 & -\frac{6}{5L} & -\frac{1}{5} & 0 & \frac{6}{5L} & 0 \\ 0 & 0 & 0 & 0 & 0 & 0 \end{bmatrix} \tag{60}$$

- Element with end A is pin connection, and end B is FR connection:

$$[k_{Gs}]_e = N\begin{bmatrix} 0 & 0 & 0 & 0 & 0 & 0 \\ 0 & \frac{6}{5L} & 0 & 0 & -\frac{6}{5L} & \frac{1}{5} \\ 0 & 0 & 0 & 0 & 0 & 0 \\ 0 & 0 & 0 & 0 & 0 & 0 \\ 0 & -\frac{6}{5L} & 0 & 0 & \frac{6}{5L} & -\frac{1}{5} \\ 0 & \frac{1}{5} & 0 & 0 & -\frac{1}{5} & \frac{L}{5} \end{bmatrix} \tag{61}$$

- Element with both ends are pin connections:

$$[k_{Gs}]_e = N\begin{bmatrix} 0 & 0 & 0 & 0 & 0 & 0 \\ 0 & \frac{1}{L} & 0 & 0 & -\frac{1}{L} & 0 \\ 0 & 0 & 0 & 0 & 0 & 0 \\ 0 & 0 & 0 & 0 & 0 & 0 \\ 0 & -\frac{1}{L} & 0 & 0 & \frac{1}{L} & 0 \\ 0 & 0 & 0 & 0 & 0 & 0 \end{bmatrix} \tag{62}$$

The geometric stiffness matrix for the special case of a beam-column element with both FR ends coincides with the geometric stiffness matrix according to Przemieniecki (1968) [38], McGuire et al. (2014) [39], Chen & Lui (1987) [2]. These stiffness matrices are used in analysis of frame structure with beam-column elements with FR or pin ends.

3. Establishing the Equivalent Nodal Load Vector for a Semi-rigid Beam-column Element

Consider a semi-rigid beam element subjected to uniformly distributed loads and concentrated loads as shown in Figure 2. This section establishes the equivalent load vector converted to a node according to FEM in local coordinate system.

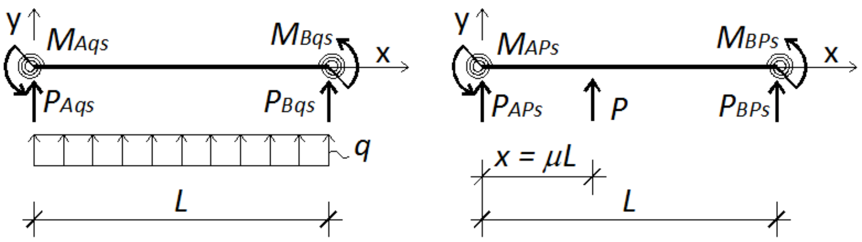

Figure 2. The load on the semi-rigid beam element is converted to nodes

3.1. Uniformly Distributed Load

From Equation 16, in case of uniformly distributed load $q(x) = q$, as shown in Figure 2-a, the equivalent nodal load vector $\{P_{qs}\}_e$ can be calculated according to the formula:

$$\{P_{qs}\}_e = q\int_0^L [N(x)]^T\,dx = q\int_0^L \begin{bmatrix} N_2(x) \\ N_3(x) \\ N_5(x) \\ N_6(x) \end{bmatrix} dx = q\int_0^L \begin{bmatrix} 1 - d_1x - 3d_2x^2 + d_3x^3 \\ d_4x - d_5x^2 + d_2x^3 \\ d_1x + 3d_2x^2 - d_3x^3 \\ -d_6x - d_7x^2 + d_8x^3 \end{bmatrix} dx \tag{63}$$

Integrating the above expression, obtaining the equivalent nodal load vector:

$$\{P_{qs}\}_e = \{P_{Aqs} \quad M_{Aqs} \quad P_{Bqs} \quad M_{Bqs}\}_e^T = q\begin{bmatrix} -\frac{d_1L^2}{2} - d_2L^3 + \frac{d_3L^4}{4} + L \\ \frac{d_2L^4}{4} + \frac{d_4L^2}{2} - \frac{d_5L^3}{3} \\ \frac{d_1L^2}{2} + d_2L^3 - \frac{d_3L^4}{4} \\ -\frac{d_6L^2}{2} - \frac{d_7L^3}{3} + \frac{d_8L^4}{4} \end{bmatrix} \tag{64}$$

Similarly, four special cases of uniformly distributed load vectors converted to nodes are determined as follows:

- Element with both ends are FR connections:

$$\{P_{qs}\}_e = \left\{\frac{qL}{2} \quad \frac{qL^2}{12} \quad \frac{qL}{2} \quad -\frac{qL^2}{12}\right\}^T \tag{65}$$

- Element with end A is FR connection, and end B is pin connection:

$$\{P_{qs}\}_e = \left\{\frac{5qL}{8} \quad \frac{qL^2}{8} \quad \frac{3qL}{8} \quad 0\right\}^T \tag{66}$$

- Element with end A is pin connection, and end B is FR connection:

$$\{P_{qs}\}_e = \left\{\frac{3qL}{8} \quad 0 \quad \frac{5qL}{8} \quad -\frac{qL^2}{8}\right\}^T \tag{67}$$

- Element with both ends are pin connections:

$$\{P_{qs}\}_e = \left\{\frac{qL}{2} \quad 0 \quad \frac{qL}{2} \quad 0\right\}^T \tag{68}$$

3.2. Concentrated Load Inside the Element

From Equation 16, in case of concentrated load P at location $x = \mu L$ as shown in Figure 2-b, the equivalent nodal load vector $\{P_{Ps}\}_e$ can be calculated according to the formula:

$$\{P_{Ps}\}_e = \{P_{APs} \quad M_{APs} \quad P_{BPs} \quad M_{BPs}\}_e^T = P[N(x)]^T = P\begin{bmatrix} N_2(\mu L) \\ N_3(\mu L) \\ N_5(\mu L) \\ N_6(\mu L) \end{bmatrix} = P\begin{bmatrix} 1 - d_1\mu L - 3d_2\mu^2L^2 + d_3\mu^3L^3 \\ d_4\mu L - d_5\mu^2L^2 + d_2\mu^3L^3 \\ d_1\mu L + 3d_2\mu^2L^2 - d_3\mu^3L^3 \\ -d_6\mu L - d_7\mu^2L^2 + d_8\mu^3L^3 \end{bmatrix} \tag{69}$$

Similarly, four special cases of concentrated load vector converted to nodes are as follows:

- Element with both ends are FR connections:

$$\{P_{Ps}\}_e = P\{2\mu^3 - 3\mu^2 + 1 \quad L(\mu^3 - 2\mu^2 + \mu) \quad -2\mu^3 + 3\mu^2 \quad L(\mu^3 - \mu^2)\}^T \tag{70}$$

- Element with end A is FR connection, and end B is pin connection:

$$\{P_{Ps}\}_e = P\left\{\frac{\mu^3}{2} - \frac{3\mu^2}{2} + 1 \quad L\left(\frac{\mu^3}{2} - \frac{3\mu^2}{2} + \mu\right) \quad -\frac{\mu^3}{2} + \frac{3\mu^2}{2} \quad 0\right\}^T \tag{71}$$

- Element with end A is pin connection, and end B is FR connection:

$$\{P_{Ps}\}_e = P\left\{\frac{\mu^3}{2} - \frac{3\mu}{2} + 1 \quad 0 \quad -\frac{\mu^3}{2} + \frac{3\mu}{2} \quad L\left(\frac{\mu^3}{2} - \frac{\mu}{2}\right)\right\}^T \tag{72}$$

- Element with both ends are pin connections:

$$\{P_{Ps}\}_e = P\{1 - \mu \quad 0 \quad \mu \quad 0\}^T \tag{73}$$

3.3. Equivalent Load Vector Converted to A Node of Semi-Rigid Beam-Column Element

Let $\{P_j\}_e$ be the concentrated load vector located at the nodes in the local coordinate system. The nodal load vector of a semi-rigid beam-column element in the local coordinate system $\{P_s\}_e$ is calculated by the formula:

$$\{P_s\}_e = \{\overline{P}_s\}_e + \{P_j\}_e \tag{74}$$

Here, $\{\overline{P}_s\}_e$ is the vector of loads placed inside the nodal element (including evenly distributed load and concentrated load) of the semi-rigid beam-column element, calculated according to the formula:

$$\{\overline{P}_s\}_e = \{P_{qs}\}_e + \{P_{Ps}\}_e \quad (75)$$

4. Set of Equilibrium Equation and Solution Method

4.1. Establishing the Set of Equilibrium Equations in Global Coordinate System

Because of the framework is made up of many different elements with different local coordinate systems, in calculations it is necessary to return to the global coordinate system. The e^{th} element in the global coordinate system $O'x'y'$ has the nodal load vector, stiffness matrix and nodal displacement vector denoted $\{P_s'\}_e$, $[k_s']_e$, $\{\delta_s'\}_e$, respectively. According to FEM, the relationship between load and displacement between two coordinate systems is determined as follows:

$$\begin{aligned}\{P_s\}_e &= [T]_e\{P_s'\}_e \\ \{\delta_s\}_e &= [T]_e\{\delta_s'\}_e\end{aligned} \quad (76)$$

wherein, $[T]_e$ is the coordinate transformation matrix, and is a square matrix, so it has orthogonal properties:

$$[T]_e^{-1} = [T]_e^T \quad (77)$$

Equation 76 can be rewritten as follows:

$$\begin{cases}\{P_s'\}_e = [T]_e^T\{P_s\}_e \\ \{\delta_s'\}_e = [T]_e^T\{\delta_s\}_e\end{cases} \quad (78)$$

Simultaneously, according to FEM, having the following formula:

$$[k_s']_e = [T]_e^T[k_s]_e[T]_e \quad (79)$$

Combining the element according to the FEM:

$$\Sigma[k_s']_e\{\delta_s'\}_e = \Sigma\{P_s'\}_e \quad (80)$$

In Equation 80, the sum sign is made according to the principles of structural combination according to FEM. Applying the boundary conditions to Equation 80, determining the system of equilibrium equations of the entire structural system in the global coordinate system:

$$[K_s^*]\{\delta_s^*\} = \{P_s^*\} \quad (81)$$

Solving the system of Equation 81, obtaining the displacements and internal forces of the semi-rigid steel frame, including the influence of the P-Delta effect.

4.2. The Method of Analyzing Semi-Rigid Steel Frames Considering the P-Delta Effect

The stiffness matrix in Equations 49 and 58 represents two nonlinear problems that need to be solved in the set of equations, including nonlinearities in the connections (if any) and nonlinearities due to the secondary P-Delta effect. Therefore, to solve Equation 81, one of several methods can be used, or a combination of nonlinear analysis methods according to Chan & Chui (2000) [5] can be used.

The linear analysis method is applied when the connection has constant stiffness. When the connection has a nonlinear model, use the pure incremental method, whereby the load is divided into many loading steps small enough to meet the convergence conditions of the method. Next, in the consideration i^{th} loading step, geometric nonlinear analysis is conducted according to the direct iterative method, whereby the stiffness matrices (depending on the change of longitudinal force) and internal forces are updated in each iterative calculation step, the convergence condition is met when the longitudinal force is approximately equal between two consecutive calculation steps. After each loading step i^{th}, the stiffness matrix, internal forces and geometric changes of the frame will be updated to serve the $(i+1)^{th}$ calculation step. In case the frame is subjected to cyclic loads, it is necessary to divide the load into even incremental steps according to the amplitude and cycle of the load. The symbols n and Eps represent the number of loading steps and and the limit variation of the axial force between two adjacent calculation steps, respectively. Similarly, the symbols N_0, N_1, and N_{max} denote the axial force of the previous calculation, the axial force of the next calculation, and the axial force of the element with the largest change in axial force value after each calculation step, respectively. A brief flowchart of the methodology process is presented in Figure 3.

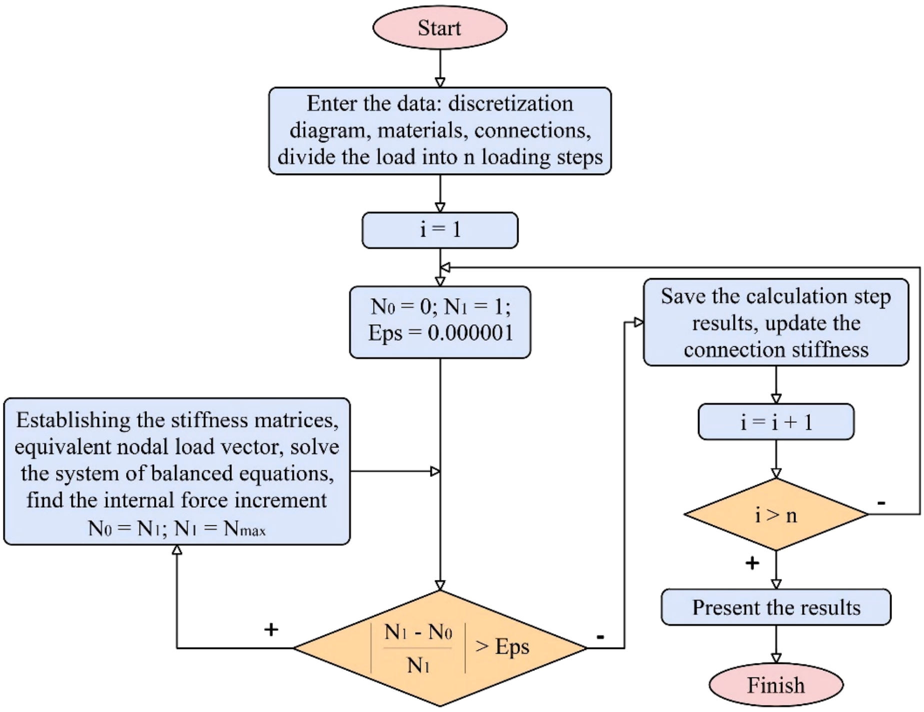

Figure 3. The second-order static analysis of semi-rigid steel frame flowchart

5. Semi-rigid Connections Modeling

Although connections can be deformed in many different forms (e.g. axial, shear, bending and torsional), only bending is considered. The behavior of the connection is expressed through the relationship between its moment and rotation. To describe the behavior of connections, various mathematical formulas have been proposed. Many experimental results have proven that the moment-rotation relationship is nonlinear. To simplify calculations, linear or multilinear models can be used. In this article, linear model, three-parameter exponential model of Kishi-Chen (1990) [40], and the four-parameter exponential model of Richard-Abbott (1975) [41] are used in Example 1, Example 2, and Example 3, respectively.

The three-parameter power model proposed by Kishi-Chen (1990) [40], includes three parameters: initial connection stiffness k_0, ultimate connection moment capacity M_u and shape parameter n, as follows:

$$M = \frac{k_0\theta}{\left[1+\left(\frac{\theta}{\theta_0}\right)^n\right]^{\frac{1}{n}}} \tag{82}$$

wherein, M and θ are respectively the moment and rotation angle at the consideration loading step of connection; $\theta_0 = M_u/k_0$ is reference plastic rotation, and the corresponding tangent stiffness of the connection is given by:

$$k = \frac{dM}{d\theta} = \frac{k_0}{\left[1+\left(\frac{\theta}{\theta_0}\right)^n\right]^{\frac{(n+1)}{n}}} \tag{83}$$

The four-parameter exponential model was proposed by Richard-Abbott (1975) [41], including four parameters: initial stiffness k_0, strain-hardening stiffness k_p, reference moment M_0 and parameter defining the sharpness of the curve n. The formula of the model is as follows:

$$M = \frac{(k_0-k_p)|\theta|}{\left[1+\left|\frac{(k_0-k_p)|\theta|}{M_0}\right|^n\right]^{\frac{1}{n}}} + k_p|\theta| \tag{84}$$

and the corresponding tangent stiffness of the connection is given by:

$$k = \left.\frac{dM}{d\theta}\right|_{|\theta|=|\theta|} = \frac{(k_0-k_p)}{\left[1+\left|\frac{(k_0-k_p)|\theta|}{M_0}\right|^n\right]^{\frac{n+1}{n}}} + k_p \tag{85}$$

6. Numerical Verification and Discussion

To validate the proposed method for establishing the shape function, stiffness matrices, and the equivalent nodal load vector for semi-rigid beam-column element, a series of numerical examples are provided. These examples are compared against published research results to verify accuracy and applicability.

6.1. Example 1 - Single-Span Two-Story Steel Frame with Linear Semi-Rigid Connection

The results of displacement and internal force of the two-story single-span steel frame in Figure 4 were calculated and verified with the SAP2000 structural analysis program, Bhatti & Hingtgen (1995) [42], Dhillon & O'Malley III (1999) [16] and Abolmaali & Choi (2004) [43]. Horizontal load H = 44.5 kN (100 $kips$), vertical load P = 444.8 kN (100 $kips$). Frame elements are erected from $W12 \times 96$ steel columns and $W14 \times 48$ steel beams, $A36$ steel according to AISC standards. Elastic modulus E = 199948.04 MPa (29000 ksi). The column bases are pin supports. The semi-rigid column-beam connection has a stiffness of 88.889 $kN.m/rad$ (786.732 $kips.in/rad$).

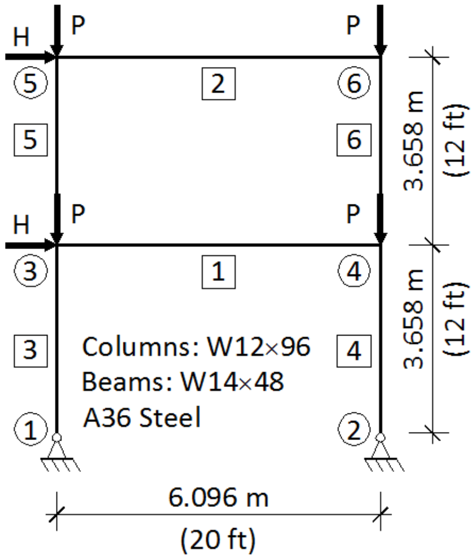

Figure 4. Single-span two-story frame with concentrated loads at the node

The programming was performed using Matlab software, the calculation results are summarized in table for comparison and verification. The results of horizontal displacement calculations at nodes 3 and 5 during first-order elastic analysis and second-order elastic analysis of a rigid frame are presented in Table 3, while the results of second-order elastic analysis of a semi-rigid frame are shown in Table 5. The maximum bending moments in each element of the frame are provided in Table 4 for first-order and second-order elastic analyses of rigid frames, and in Table 6 for second-order elastic analysis of semi-rigid frames.

Table 3. Horizontal displacement of rigid frame (mm), Example 1

Node #	Rigid frame, elastic-first order		Rigid frame, elastic-second order					
	Bhatti & Hingtgen [42]	Present study	SAP 2000	Bhatti & Hingtgen [42] (A)	Dhillon & O'Malley III [16]	Abolmaali & Choi [43]	Present study (B)	(B-A)/(A) (%)
3	25.7	25.6896	25.691	29.7	29.6	29.7	29.6890	-0.04%
5	38.3	38.3513	38.354	44.0	43.8	44.0	43.9818	-0.04%

Table 4. Maximum bending moment of rigid frame (kN.m), Example 1

Member #	Rigid frame, elastic-first order		Rigid frame, elastic-second order					
	Bhatti & Hingtgen [42]	Present study	SAP 2000	Bhatti & Hingtgen [42] (A)	Dhillon & O'Malley III [16]	Abolmaali & Choi [43]	Present study (B)	(B-A)/(A) (%)
1	163.8	163.8852	187.17	186.9	186.8	187.1	187.1927	0.16%
2	80.3	80.3692	89.81	89.8	89.8	89.8	89.8144	0.02%
3	163.0	163.1010	189.57	189.5	189.4	189.5	189.5958	0.05%
4	162.4	162.4610	188.7	188.6	188.6	188.6	188.7185	0.06%
5	80.3	80.3224	89.76	89.7	89.7	89.7	89.7674	0.08%
6	80.3	80.3692	89.81	89.8	89.8	89.8	89.8144	0.02%

Table 5. Horizontal displacement of semi-rigid frame (mm), Example 1

Node #	Semi-rigid frame, elastic-second order					
	SAP 2000	Bhatti & Hingtgen [42] (A)	Dhillon & O'Malley III [16]	Abolmaali & Choi [43]	Present study (B)	(B-A)/(A) (%)
3	37.534	37.5	37.4	37.5	37.5378	0.10%
5	58.233	58.2	58.1	58.2	58.2318	0.05%

Table 6. Maximum bending moment of semi-rigid frame (kN.m), Example 1

Frame #	Semi-rigid frame, elastic-second order					
	SAP 2000	Bhatti & Hingtgen [42] (A)	Dhillon & O'Malley III [16]	Abolmaali & Choi [43]	Present study (B)	(B-A)/(A) (%)
1	184.86	184.6	184.6	184.8	184.9128	0.17%
2	101.93	101.9	101.9	101.9	101.9183	0.02%
3	196.55	196.5	196.4	196.5	196.5903	0.05%
4	195.67	195.6	195.5	195.7	195.6889	0.05%
5	101.89	101.9	101.9	101.8	101.8970	0.00%
6	101.93	101.9	101.9	101.9	101.9183	0.02%

Verification shows that the calculation results of the present study closely align with the results published in the above references, particularly those by Bhatti & Hingtgen [42]. Thus, it can be seen that the proposed analysis method according to the present theory is reliable.

6.2. Example 2 - Single-Span Two-Story Steel Frame with Nonlinear Semi-Rigid Connection

According to Chan & Chui [5], Stelmack (1982) [1] tested the behavior of a two-story single-span steel frame with concentrated static load as shown in Figure 5. This steel frame was chosen as the benchmark frame for verification in the study of Kim & Choi (2001) [17], and this study. Frame elements are erected from $W12 \times 96$ steel columns and $W14 \times 48$ steel beams, $A36$ steel according to AISC standards. Elastic modulus E = 199948.04 MPa (29000 ksi). The column bases are pin supports. The semi-rigid beam-column connection is made of $A325$, $3/4$ in bolts and $A36$, $L4 \times 4 \times 1/2$ in angle steel, at the upper and lower flanges of the beam. The concentrated load in gravity direction on the first floor beam span P_1 = 10.68 kN (2.4 $kips$) was first applied at third points of the beam, and then two horizontal loads act together, proportionally.

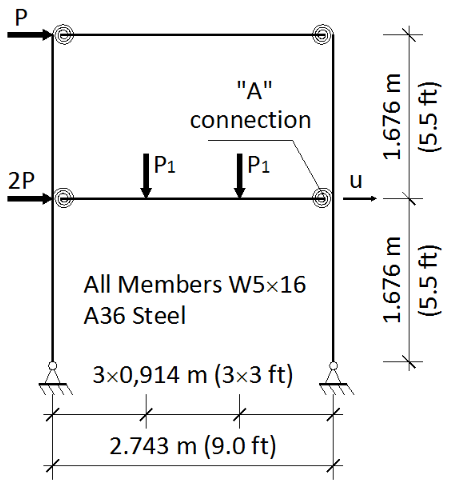

Figure 5. Two-story, single-span frame with concentrated static load according to Stelmack's experiments

In Figure 6, the load-horizontal displacement curve (u) at the first floor almost coincides with the experimental results of Stelmack (1982) [1]. In Figure 7, the moment-rotation curve in connection A is very close to the theoretical calculation results obtained using Explicit Equations (the parameters of the semi-rigid connection model were calculated according to the formula, depending on the type of semi-rigid connection) by Kim & Choi (2001) [17], and there is a small degree of difference compared with the moment-rotation curve from the experiment. Thus, it can be seen that the proposed calculation method according to the present theory is reliable.

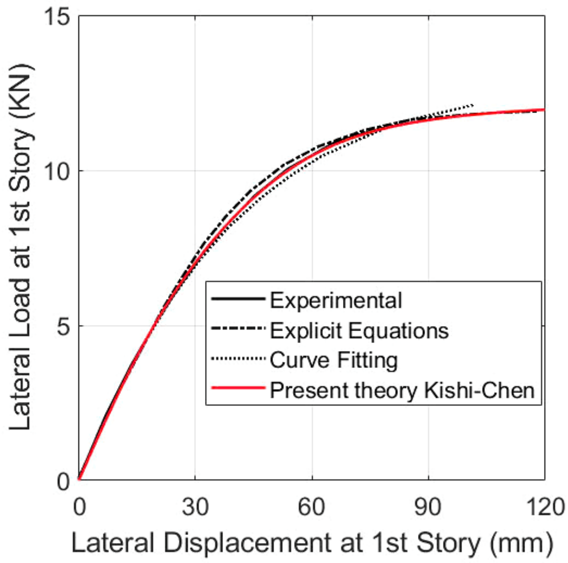

Figure 6. Comparison of the load-horizontal displacement curve u at the 1st story for verification study

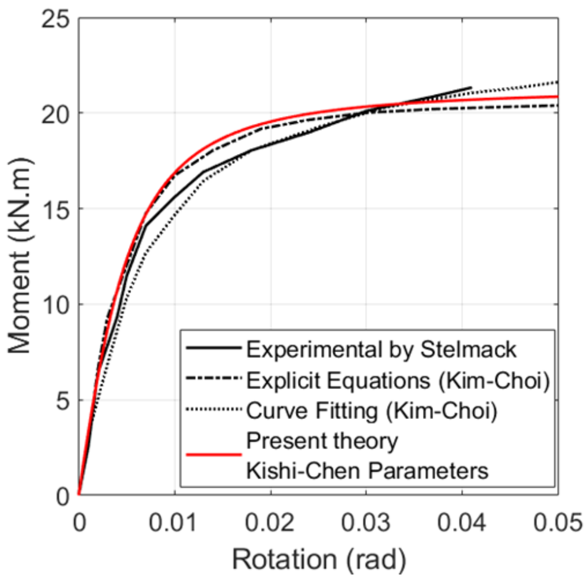

Figure 7. Comparison of the moment-rotation curve at A connection for verification study

The relationship between horizontal load P and horizontal displacement u at first story, and relationship between moment-rotation at A connection are calculated and verified with the experiments of Stelmack (1982) [1], and Kim & Choi (2001) [17]. The beam-column connections according to Kishi-Chen (1987) exponential model with three parameters including: $k_0 = 3373.16 kN.m/rad$ ($29855 kips.in/rad$), $M_u = 20.90 kN.m$ ($185 kips.in$), $n = 1.65$. After programming with Matlab software, the calculation results are shown in Figures 6 and 7.

6.3. Example 3 - Single-Span Two-Story Steel Frame with Nonlinear Semi-Rigid Connection, Cyclic Loads

In this example, the two-story single-span steel frames with cyclic lateral load steel frame tested by Stelmack et al. (1986) [44] was used for validation calculations. The structure of the frame is stated in Example 2. The frame is subjected to cyclic lateral load with load increment equal to $\pm 4.45 kN (\pm 1.0 kips)$ and increased up to $\pm 22.24 kN (\pm 5.0 kips)$. For the second story, the load is always one-half of the load at first story. Frame model, cycle load history, experimental results and moment-rotation relationship curve in the connection according to the Richard-Abbott model in Figure 8.

Calculation to verify the framework according to the experiments of Stelmack et al. (1986) [44], Chan & Chui (2000) [5], and Valipour & Bradford (2013) [45]. The beam-column connections according to the Richard-Abbott (1975) [41] exponential model with four parameters including: $k_0 = 2372.68 kN.m/rad$ ($21000 kips.in/rad$), $k_p = 135.58 kN.m/rad$ ($1200 kips.in/rad$), $M_0 = 15.82 kN.m$ ($140 kips.in$), $n = 1.8$.

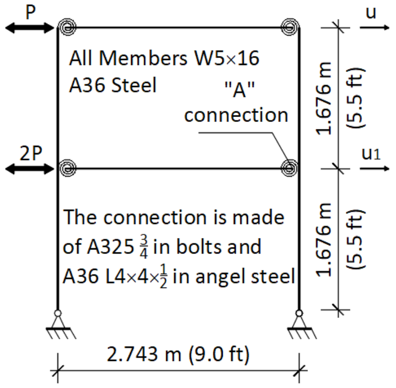

a) Steel frame calculation model

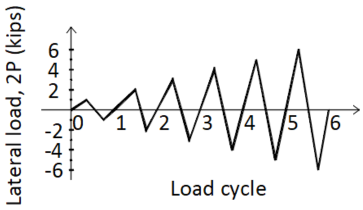

b) Lateral load history

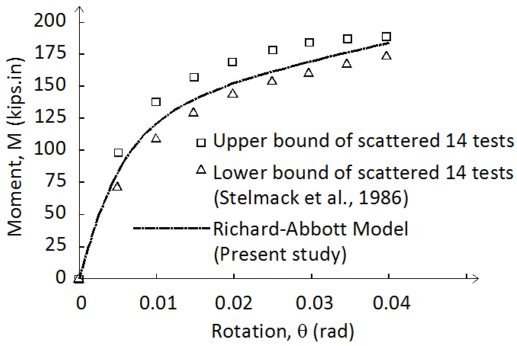

c) Moment-rotation angle relationship of experimental connection by Stelmack (1986) [44] and by Richard-Abbott model (1975) [41]

Figure 8. Two-story, single-span frame with cyclic lateral load according to Stelmack's experiments

In the frame, each beam or column member is simulated with only one semi-rigid beam-column element as established. After programming with Matlab software to calculate using the FEM, we obtained the analysis results as follows: horizontal displacement curve u at the second-story and load P with cycle 2 and cycle 3 as shown in Figure 9, the horizontal displacement curve u_1 at the first-story and the load P are as shown in Figure 10, and the moment-rotation angle relationship curve in connection A is as shown in Figure 11. The total load application procedure is divided into 6,000 steps.

It can be observed in Figures 9 to 11 that the displacement and force responses obtained from the analysis of the present theory show a strong correlation with the experimental results and the theoretical calculation results of other authors. The results of the present theory are quite close to the experimental results. The discrepancy between the results of the present theory and those of other studies may be due to the application of the semi-rigid connection behavior model or the use of different computational programming techniques. The loading/unloading model can exert a local or global effect on the frame structure subjected to cyclic loads. Thus, it can be seen that the proposed calculation method based on the present theory is reliable.

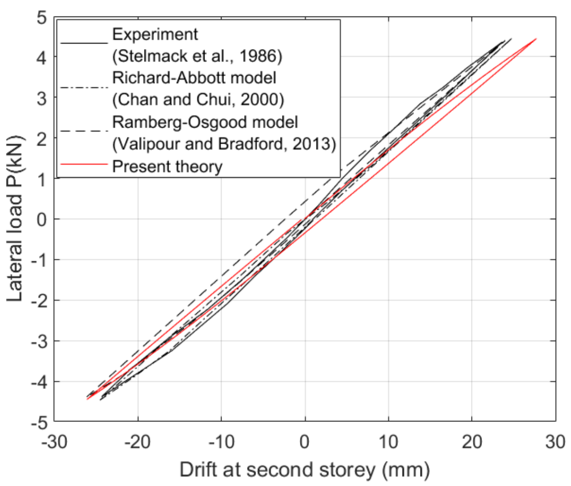

a) Cycle 2

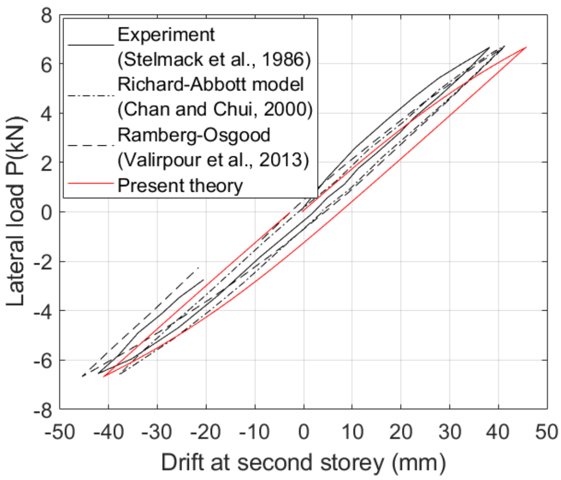

b) Cycle 3

Figure 9. P-u Relationship

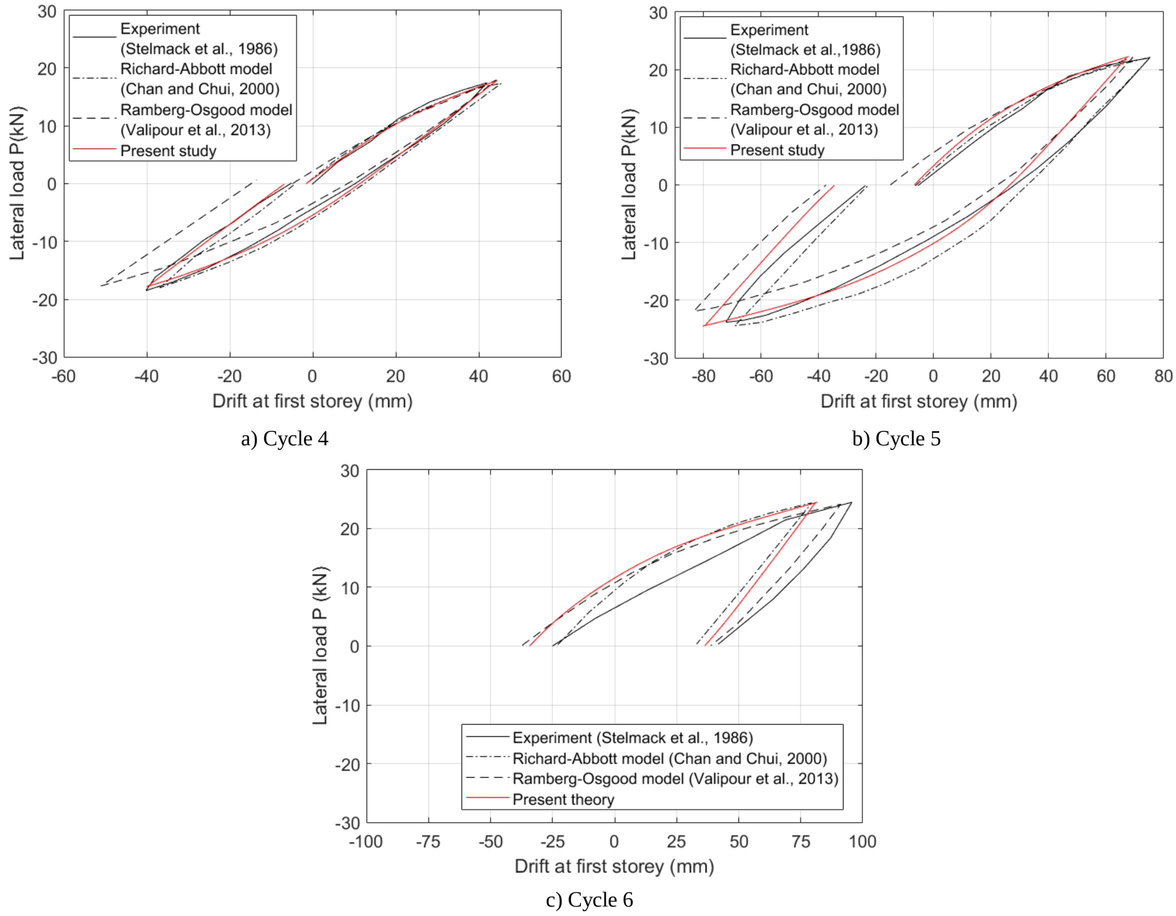

Figure 10. P-u1 Relationship

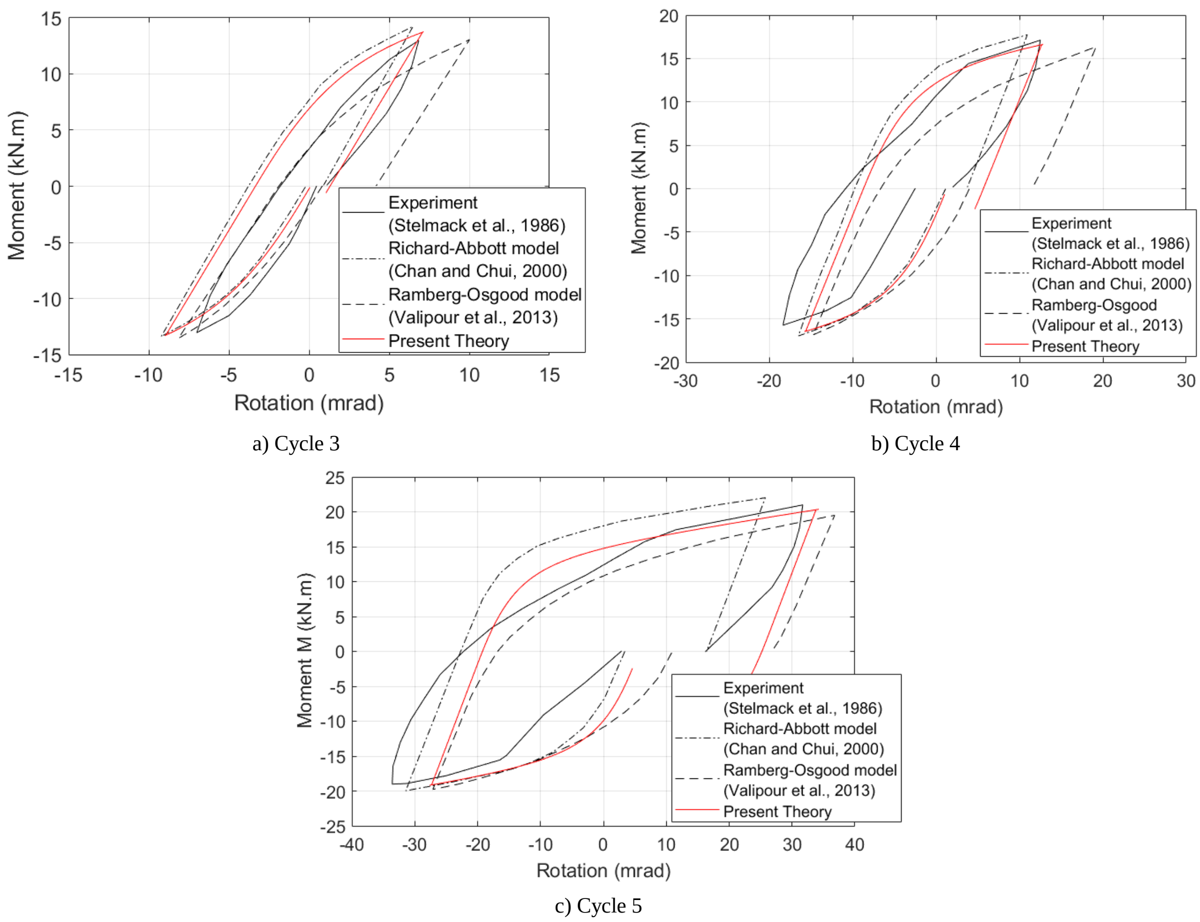

Figure 11. Relationship between moment-rotation angle in connection A

7. Conclusions

This paper has presented a novel method for establishing the shape functions for semi-rigid beam-column element in the second-order analysis of steel frames. The proposed method offers a comprehensive framework for developing stiffness matrices that effectively account for both the P-Delta effect and the flexibility of semi-rigid connections. The key findings and contributions of this study are summarized as follows:

1. ***Shape Function Development:*** The shape functions for semi-rigid beam-column element were derived based on the geometric properties of the element and the stiffness of its connections. The resulting shape functions are expressed as polynomials, facilitating straightforward calculation and implementation within the finite element method (FEM).
2. ***Stiffness Matrices:*** The linear elastic stiffness matrix and the geometric stiffness matrix for semi-rigid beam-column element were derived using Castigliano's theorem (Part 1). These matrices are crucial for accurate second-order analysis, effectively capturing the influence of semi-rigid connections on the overall structural response.
3. ***Equivalent Nodal Load Vectors:*** The equivalent nodal load vectors for the semi-rigid beam-column element were derived from the established shape functions and the FEM. These vectors are essential for calculating loads applied to the element, converted to nodal forces in the analytical model.
4. ***Special Cases:*** The proposed method was successfully applied to special cases, including fully rigid (FR) and pinned connections. The resulting stiffness matrices and equivalent nodal load vectors for these scenarios were simplified, demonstrating the method's flexibility and applicability to various connection types.
5. ***Numerical Verification:*** The proposed method was validated through several numerical examples, investigating steel frames with semi-rigid connections as benchmark cases. These frameworks, widely recognized for validation, showed excellent agreement with analytical solutions, published research, and finite element analysis (FEA) simulations, confirming the accuracy and robustness of the proposed approach.
6. ***Practical Applications:*** The method is well-suited for practical applications in structural engineering, particularly in the design and analysis of steel frames with semi-rigid connections. By accounting for both the connection flexibility and P-Delta effects, the proposed approach provides a more realistic and reliable analysis framework for modern steel structures.

In conclusion, the new method for establishing shape functions and stiffness matrices for semi-rigid beam-column element offers significant advantages in the second-order analysis of steel frames. Future research could explore further applications of this method to more complex structural systems and the integration of non-linear material behavior.

8. Declarations

8.1. Author Contributions

Conceptualization, L.D.B.T.; methodology, V.Q.A.; software, N.H.Q.; validation, V.Q.A.; formal analysis, L.D.B.T.; investigation, V.Q.A., L.D.B.T., and N.H.Q.; resources, L.D.B.T.; data curation, L.D.B.T.; writing—original draft preparation, L.D.B.T. and N.H.Q.; writing—review and editing, V.Q.A.; supervision, V.Q.A.; project administration, V.Q.A. All authors have read and agreed to the published version of the manuscript.

8.2. Data Availability Statement

The data presented in this study are available in the article.

8.3. Funding

The authors received no financial support for the research, authorship, and/or publication of this article.

8.4. Conflicts of Interest

The authors declare no conflict of interest.

9. References

[1] Stelmack, T. W. (1982). Analytical and experimental response of flexibly-connected steel frames. Master Thesis, University of Colorado, Boulder, United States.

[2] Chen, W. F. & Lui, E. M. (1987). Structural stability theory and implementation. Elsevier, Amsterdam, Netherlands.

[3] Anh, V. Q. (2003). Research on analysis and calculation methods of steel frames with elastic connections. Ph.D. Thesis, Hanoi University of Architecture, Hanoi, Vietnam. (In Vietnamese).

[4] Quang, N. H. (2012). Calculation of steel frames with semi-rigid connections according to the elastic-plastic model subjected to dynamic loads. PhD Thesis, Hanoi University of Architecture, Hanoi, Vietnam. (In Vietnamese).

[5] Chan, S. L., & Chui, P. T. (2000). Non-linear static and cyclic analysis of steel frames with semi-rigid connections. Elsevier, Amsterdam, Netherlands.

[6] LRFD (AISC). (2000). Load and Resistance Factor Design Specification for Structural Steel Buildings. American Institute of Steel Construction (AISC), Chicago, United States.

[7] EN 1993-1-1 (CEN) (2005). Design of steel structures - Part 1-1: General rules and rules for buildings. European Committee for Standardization, Brussels, Belgium.

[8] Monforton, G. R. (1962). Matrix analysis of frames with semi-rigid connections, Master Thesis. University of Windsor, Ontario, Canada.

[9] Dhillon, B. S., & Abdel-Majid, S. (1990). Interactive analysis and design of flexibly connected frames. Computers and Structures, 36(2), 189–202. doi:10.1016/0045-7949(90)90118-L.

[10] Xu, L., & Grierson, D. E. (1993). Computer-Automated Design of Semirigid Steel Frameworks. Journal of Structural Engineering, 119(6), 1740–1760. doi:10.1061/(asce)0733-9445(1993)119:6(1740).

[11] Xu, L. (2001). Second-order analysis for semirigid steel frame design. Canadian Journal of Civil Engineering, 28(1), 59–76. doi:10.1139/l00-077.

[12] Lui, E. M., & Chen, W. F. (1986). Analysis and behaviour of flexibly-jointed frames. Engineering Structures, 8(2), 107–118. doi:10.1016/0141-0296(86)90026-X.

[13] Xu, L. (1992). Geometrical stiffness and sensitivity matrices for optimization of semi-rigid steel frameworks. Structural Optimization, 5(1–2), 95–99. doi:10.1007/BF01744701.

[14] Chen, W. F. (2000). Practical Analysis for Semi-Rigid Frame Design. World Scientific, Singapore. doi:10.1142/4277.

[15] Bazant, Z. P., & Cedolin, L. (2010). Stability of structures: elastic, inelastic, fracture and damage theories. World Scientific, Singapore. doi:10.1142/9789814317047.

[16] Dhillon, B. S., & O'Malley III, J. W. (1999). Interactive Design of Semirigid Steel Frames. Journal of Structural Engineering, 125(5), 556–564. doi:10.1061/(asce)0733-9445(1999)125:5(556).

[17] Kim, S. E., & Choi, S. H. (2001). Practical advanced analysis for semi-rigid space frames. International Journal of Solids and Structures, 38(50–51), 9111–9131. doi:10.1016/S0020-7683(01)00141-X.

[18] Nguyen, P. C., & Kim, S. E. (2014). An advanced analysis method for three-dimensional steel frames with semi-rigid connections. Finite Elements in Analysis and Design, 80, 23–32. doi:10.1016/j.finel.2013.11.004.

[19] Chan, S. L., & Ho, G. W. M. (1994). Nonlinear Vibration Analysis of Steel Frames with Semirigid Connections. Journal of Structural Engineering, 120(4), 1075–1087. doi:10.1061/(asce)0733-9445(1994)120:4(1075).

[20] Chan, S. L. (1994). Vibration and modal analysis of steel frames with semi-rigid connections. Engineering Structures, 16(1), 25–31. doi:10.1016/0141-0296(94)90101-5.

[21] Chui, P. P. T., & Chan, S. L. (1997). Vibration and deflection characteristics of semi-rigid jointed frames. Engineering Structures, 19(12), 1001–1010. doi:10.1016/s0141-0296(97)00126-0.

[22] Suarez, L. E., Singh, M. P., & Matheu, E. E. (1996). Seismic response of structural frameworks with flexible connections. Computers and Structures, 58(1), 27–41. doi:10.1016/0045-7949(95)00108-S.

[23] Sekulovic, M., & Salatic, R. (2001). Nonlinear analysis of frames with flexible connections. Computers and Structures, 79(11), 1097–1107. doi:10.1016/S0045-7949(01)00004-9.

[24] Zohra, D. F., & Nacer, I. T. A. (2018). Dynamic analysis of steel frames with semi-rigid connections. Structural Engineering and Mechanics, 65(3), 327–334. doi:10.12989/sem.2018.65.3.327.

[25] Salatic, R. (2019). Seismic analysis of steel frames with semi-rigid and viscous connections. 7th International Conference Contemporary achievements in civil engineering, 23-24 April, 2019, Subotica, Serbia.

[26] Zlatkov, D. (2015). Theoretical and experimental analysis of reinforced concrete frame structures with semi-rigid connections. Ph.D. Thesis, University of Niš, Niš, Serbia. (In Serbian).

[27] Milićević, M. (1986). Design of systems with semi-rigid connections by use of slope-deflection method. 17th Yugoslav Congress of Theoretical And Mechanics, Zadar, Croatia.

[28] Zlatkov, D., Zdravkovic, S., Mladenovic, B., & Stojic, R. (2011). Matrix formulation of dynamic design of structures with semi-rigid connections. Facta Universitatis - Series: Architecture and Civil Engineering, 9(1), 89–104. doi:10.2298/fuace1101089z.

[29] Zlatkov, D., Zdravkovic, S., Mladenovic, B., & Mijalkovic, M. (2020). Seismic analysis of frames with semi-rigid connections in accordance with EC8. Facta Universitatis - Series: Architecture and Civil Engineering, 18(2), 203–217. doi:10.2298/fuace201208015z.

[30] Anh, V. Q. (2002). Stability analysis of steel frames with semi-rigid connections and rigid zones by using P-Delta effect. Vietnam Journal of Mechanics, 24(1), 14–24. doi:10.15625/0866-7136/24/1/6605.

[31] Anh, V. Q. (2002). Analysis plane steel frame with semi-rigid connections and rigid-zones with consideration of the second order effect. Advances in Building Technology, II, 1043–1049. doi:10.1016/b978-008044100-9/50131-5.

[32] Nguyen, P.-C., Tran, T.-T., & Nghia-Nguyen, T. (2021). Nonlinear time-history earthquake analysis for steel frames. Heliyon, 7(8), e06832. doi:10.1016/j.heliyon.2021.e06832.

[33] Dang, H. K., Thai, D. K., & Kim, S. E. (2023). Stochastic analysis of semi-rigid steel frames using a refined plastic-hinge model and Latin hypercube sampling. Engineering Structures, 291(116313), 1–16. doi:10.1016/j.engstruct.2023.116313.

[34] De Souza, L. A. F., & Verdade, L. L. (2023). Numerical-Computational Model for Dynamic Nonlinear Analysis of Frames With Semi-Rigid Connection Considering the Damping Effect. Revista de Gestão Social e Ambiental, 18(1), e04192. doi:10.24857/rgsa.v18n1-019.

[35] Saadi, M., Yahiaoui, D., Lahbari, N., & Tayeb, B. (2021). Seismic fragility curves for performance of semi-rigid connections of steel frames. Civil Engineering Journal (Iran), 7(7), 1112–1124. doi:10.28991/cej-2021-03091714.

[36] Genovese, F., & Sofi, A. (2024). A novel interval matrix stiffness method for the analysis of steel frames with uncertain semi-rigid connections. Advances in Engineering Software, 192, 103629. doi:10.1016/j.advengsoft.2024.103629.

[37] Jough, F. K. G., & Soori, M. (2024). Considering the Effect of Semi-Rigid Connection in Steel Frame Structures for Progressive Collapse. World Academy of Science, Engineering and Technology International Journal of Structural and Construction Engineering, 18(6), 218–227.

[38] Przemieniecki, J. S. (1985). Theory of matrix structural analysis. Courier Corporation, North Chelmsford, United States.

[39] McGuire, W., Gallagher, R. H., & Saunders, H. (2014). Matrix Structural Analysis. John Wiley & Sons, Hoboken, United States.

[40] Kishi, N., & Chen, W. F. (1990). Moment-rotation relations of semirigid connections with angles. Journal of Structural Engineering, 116(7), 1813-1834. doi:10.1061/(ASCE)0733-9445(1990)116:7(1813).

[41] Richard, R. M., & Abbott, B. J. (1975). Versatile elastic-plastic stress-strain formula. Journal of the Engineering Mechanics Division, 101(4), 511-515. doi:10.1061/JMCEA3.0002047.

[42] Bhatti, M. A., & Hingtgen, J. D. (1995). Effects of connection stiffness and plasticity on the service load behavior of unbraced steel frames. Engineering Journal, 32(1), 21–33. doi:10.62913/engj.v32i1.637.

[43] Abolmaali, A., & Choi, Y. (2004). Nonlinear moment reversal behavior in steel frames. Korean Science Journal, Korea Spatial Information Society (KSIS), 5(22), 3-15.

[44] Stelmack, T. W., Marley, M. J., & Gerstle, K. H. (1986). Analysis and tests of flexibly connected steel frames. Journal of Structural Engineering, 112(7), 1573-1588. doi:10.1061/(ASCE)0733-9445(1986)112:7(1573).

[45] Valipour, H. R., & Bradford, M. A. (2013). Nonlinear P-Δ analysis of steel frames with semi-rigid connections. Steel & Composite Structures, 14(1), 1–20. doi:10.12989/scs.2013.14.1.001.